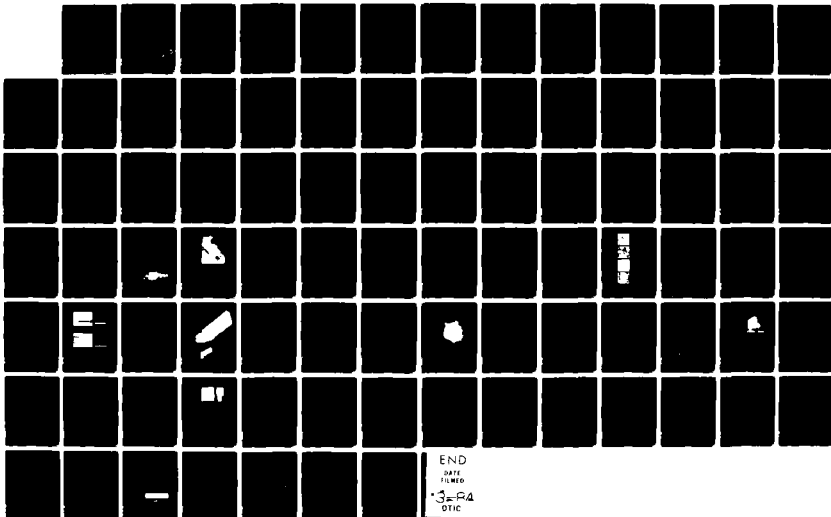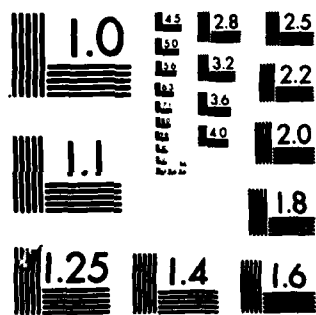AD-A137 350   INVESTIGATION OF NEW CONCEPTS FOR DESIGNING   1/1
               MILLIMETRE-WAVE ANTENNAS(U) ROYAL MILITARY COLL OF
               SCIENCE SHRIVENHAM (ENGLAND)   J R JAMES ET AL. SEP 83
UNCLASSIFIED   DAJA37-80-C-0183   F/G 9/5   NL

END
DATE
FILMED
3-84
DTIC

MICROCOPY RESOLUTION TEST CHART
NATIONAL BUREAU OF STANDARDS-1963-A

type / 84-6

AD A137350

AD

INVESTIGATION OF NEW CONCEPTS FOR DESIGNING MILLIMETRE-WAVE ANTENNAS

Final Technical Report

by

J.R. JAMES and C.M. HALL

SEPT 1983

United States Army

RESEARCH & STANDARDIZATION GROUP (EUROPE)

London   England

CONTRACT NUMBER . DAJA. 37-80-C-0183. .

Royal Military College of Science
Shrivenham, Nr Swindon, England

Approved for Public Release; distribution unlimited

84 01 30 087

REPORT DOCUMENTATION PAGE	READ INSTRUCTIONS BEFORE COMPLETING FORM

1. REPORT NUMBER	2. GOVT ACCESSION NO.	3. RECIPIENT'S CATALOG NUMBER
	AD-A137 350	

4. TITLE (and Subtitle)	5. TYPE OF REPORT & PERIOD COVERED
Investigation of New Concepts for Designing Millimetre-Wave Antennas	Final Technical Report June 80 - Sept 83
	6. PERFORMING ORG. REPORT NUMBER

7. AUTHOR(s)	8. CONTRACT OR GRANT NUMBER(s)
J.R. James and C.M. Hall	DAJA37-80-C-0183

9. PERFORMING ORGANIZATION NAME AND ADDRESS	10. PROGRAM ELEMENT, PROJECT, TASK AREA & WORK UNIT NUMBERS
Royal Military College of Science Shrivenham, Nr Swindon, England	6.11.02A 1T161102BH57-03

11. CONTROLLING OFFICE NAME AND ADDRESS	12. REPORT DATE
USARDSG-UK Box 65, FPO NY 09510	Sept 1983
	13. NUMBER OF PAGES
	80

14. MONITORING AGENCY NAME & ADDRESS(if different from Controlling Office)	15. SECURITY CLASS. (of this report)
	Unclassified
	15a. DECLASSIFICATION/DOWNGRADING SCHEDULE

16. DISTRIBUTION STATEMENT (of this Report)

Approved for Public Release; distribution unlimited

17. DISTRIBUTION STATEMENT (of the abstract entered in Block 20, if different from Report)

18. SUPPLEMENTARY NOTES

19. KEY WORDS (Continue on reverse side if necessary and identify by block number)

Millimetre microstrip antenna arrays, Loss mechanisms

20. ABSTRACT (Continue on reverse side if necessary and identify by block number)

The problem associated with the design of microstrip antennas and arrays at millimetre wavelengths is addressed and the dominant difficulties identified as line loss, tolerance effects and integration or connection of the antenna to the rest of the equipment using launching transitions. Several types of the latter are evaluated and measured to illustrate loss and cross-polarisation effects. Methods for reducing line loss are investigated but the reductions are not significant. The findings are summarised and related to current military requirements. An alternative structure, the hybrid microstrip —

DD FORM 1473 EDITION OF 1 NOV 65 IS OBSOLETE

20. Contd.

dielectric array is described and in principle enables array feeder loss
to be appreciably reduced but launcher loss remains the major obstacle.
Conclusions and recommendations are given and it is evident that microstrip
continues to be attractive for some military applications where planar
conformal smaller size arrays are required.

ABSTRACT

The problem associated with the design of microstrip antennas and
arrays at millimetre wavelengths is addressed and the dominant difficulties
identified as line loss, tolerance effects and integration or connection
of the antenna to the rest of the equipment using launching transitions
Several types of the latter are evaluated and measured to illustrate loss
and cross-polarisation effects. Methods for reducing line loss are
investigated but the reductions are not significant. The findings are
summarised and related to current military requirements. An alternative
structure the hybrid microstrip dielectric array is described and in
principle enables array feeder loss to be appreciably reduced but launcher
loss remains the major obstacle. Conclusions and recommendations are given
and it is evident that microstrip continues to be attractive for some
military applications where planar conformal smaller size arrays are
required.

Key words: millimetre microstrip antenna arrays, loss mechanisms.

PRINCIPAL SYMBOLS

A	Aperture Area.
a	Round conductor radius.
α	Attenuation constant.
α_c, α_{CR}	Smooth and rough conductor attenuation constants.
b	Distance of round conductor centre to ground plane.
β	$2\pi/\lambda_g$.
c	Half Insular guide width.
D	Largest aperture dimension.
d	Insular guide height, also patch separation distance.
Δ	r.m.s. surface roughness.
δ	skin depth.
η	Radiation/launching efficiency.
f	Frequency.
h	Substrate height.
I	Current.
$J_1(x)$, $J_2(x)$	Current density as a function of transverse displacement from the centre of a microstrip line for the conductor and ground plane respectively.
k_o	$2\pi/\lambda_o$.
ℓ	length.
ℓ_t	terminal load loss.
ℓ_g	feeder loss.
ℓ_ℓ	launcher loss.
λ_o	Free space wavelength.
λ_m	Microstrip wavelength.
λ_g	Insular guide wavelength.

μ_o	Permeability of free space.
N_λ	Number of wavelengths.
p	Integer.
q	Integer.
Q	Loss factor
Q_r, Q_c, Q_d	Radiation, conductor and dielectric loss factors.
R_{s1}, R_{s2}	Surface skin resistivity (Ohms per square unit) for conductor and ground plane respectively.
σ	Conductivity.
w	Width.
x	Transverse displacement from a transmission line.
x_o	Transverse displacement of a conductor from the centre of an insular guide transmission line.
Z_m	Microstrip impedance.
E^y_{11}, E^x_{21}	Insular guide modes.
ϵ_o, ϵ_r, ϵ_e	free space, relative and effective permittivities.
$\vec{E}_L$, $\vec{H}_L$	Launcher fields.
$\vec{E}_m$, $\vec{H}_m$	Microstrip fields.
$\vec{E}_I$, $\vec{H}_I$	Dielectric guide fields.
ϵ_{r1}, ϵ_{r2}	Relative dielectric constant of the substrate and overlayed guide for the insular guide structure.
P_I	Total power flowing in Insular guide.
B_{pq}	Microstrip patch modal amplitude (p and q positive integers).
k_{pq}	Wave number of microstrip patch mode.

TABLE OF CONTENTS

1. INTRODUCTION

During the past decade microstrip antennas[1,2] have developed into
a major field of activity and their advantages are well known. The
concept enables less bulky, lighter, cheaper antenna assemblies to be
created and their thin planar geometry is ideal for conformal applica-
tions and integration with circuit elements. When designers have
attempted to realise these advantages, several disadvantages have
become evident and are now widely appreciated. The high power losses
in microstrip antenna arrays and their narrow bandwidths were immediately
apparent while problems in sidelobe level control and more recently
cross-polarisation effects[3] are very much a function of the particular
application requirements.

At millimetre wavelengths microstrip antennas in principle function
in much the same way as at microwave frequencies but their realisation
is more dependent on manufacturing tolerances and increased losses.
While the manufacturing tolerances associated with the substrate and
conductor elements are significant particularly at 90 GHz and above, it
is the increased losses that have emerged as the most problematical
issue. A situation has persisted for several years now where designers
tacitly assume that microstrip antennas are likely to be too lossy at
millimetre wavelengths yet have no viable alternative for certain
applications requiring conformal, integrable, radiating structures.
Designers have been 'left in the air' not really knowing whether new
classes of antennas will emerge or whether more performance can be
squeezed out of microstrip antennas. This state-of-affairs was reflected
in earlier discussions[4] on millimetre waveguides and again, more
recently in communications[5] to the author from the US Army ERO.

The aim of this research contract is to bring about a clarification
of the potential of millimetre microstrip antennas by way of a coherent
investigation of the fundamental behaviour. As mentioned above it is the
loss mechanisms that require most attention.

To relate the findings to the requirements[5] of the US Army and
Airforce we note some of the likely millimetre wave application areas.
Aircraft mounted satellite antennas, vehicle mounted antennas and man-
portable systems are examples where the antenna is supported on an
electrically large platform. For these applications a large array can be
accommodated consisting of many elements. When the platform is electrically
small as in the case of a small missile or artillery shell or aircraft
pod etc the interest may lie in small arrays comprised of only a few
elements. Good antenna efficiency (low loss) is likely to be a requisite
for all applications whereas very wide bandwidths may only be important
for some applications such as radiometry.

In the pursuance of this programme of work we have become aware of
the dearth of quantifiable information about microstrip behaviour at
millimetre wavelengths and in many instances a confused situation exists
over the physical mechanisms occurring. This is particularly marked for
dissipative losses in microstrip lines but is also apparent regarding

the totality of radiation effects associated with microstrip antennas. The problems associated with the connection of the antenna to a compatible feed system are significant and the cross-polarisation properties are virtually unknown and have only recently received attention for some specific antenna structures. For these reasons much of the contract work has dwelt on making a thorough examination of microstrip itself together with a few antenna types and this has involved a comprehensive measurement programme. The frequency bands of interest in military systems have been chosen for the experiments and have been focussed on the 90 GHz region. Bearing in mind the fundamental nature of this work we have been able to economise in effort by experimenting on antennas such as the comb array[1] that has already had considerable design effort expended on it at microwave frequencies and computer programmes associated with manufacture already exist within the research group.

The salient findings of the programme of research are presented in the main text as follows while some supporting information is placed in appendices. This includes some administrative and other relevant details of interest which are listed in appendix 9.1. In section 2 the up-to-date situation on how to choose a substrate for microwave microstrip antennas is addressed prior to the additional problem of scaling down the dimensions for millimetre operation. This section clarifies the present microwave design procedures and identifies the difficulties that are to be investigated later on. A detailed study of launcher radiation effects is reported in section 3 while the major problem of microstrip line loss is dealt with in section 4. These two sections account for much of the fundamental work; measurement details are summarised in appendix 9.2 and a short appraisal of the current literature on loss mechanisms in lines is given in appendix 9.3. The realistic performance obtainable when all these effects are taken into consideration is illustrated in section 5 which usefully interprets the prospects for typical classes of antennas currently of interest to both the US Army and Airforce. The question which follows on from here is whether some of the advantages of microstrip antennas can be traded to bring about a different structure with acceptable performance. The replacement of microstrip feeders with dielectric lines is considered to be well worth investigating and a detailed study is reported in section 6. Overall conclusions and recommendations to the entire research programme are given in section 7.

2. CHOICE OF SUBSTRATE AND DIMENSIONAL SCALING PROBLEMS AT MILLIMETRE WAVELENGTHS

2.1 Substrates

In principle microwave microstrip antennas can be scaled down in size to function at millimetre wavelengths and since it is easier to make measurements at microwave this seems a good design procedure. Many doubts have existed on how to start off microstrip antenna design at microwave frequencies and it is only recently that the optimal choice of substrate dimensions was examined[6] for a rectangular patch antenna; the salient points are as follows and can be regarded as a good initial design guide for any type of microstrip antenna. The relationship between relative permittivity ε_r, substrate height h, bandwidth Δf and efficiency η is shown in Fig 1 while the less well known effects of substrate surface wave generation and cross polarisation on the antenna radiation pattern are embraced in Fig 2. The factor S is the ratio of radiation power to the power lost in substrate surface waves and is a pessimistic assessment of the unwanted sidelobe level that could arise in an array of such patches. Thus S is based on the assumption that the entire substrate surface wave power is re-radiated at the edge of the antenna substrate or other discontinuities in its path, to create an unwanted sidelobe. In practice these unwanted sources of radiation will not be in phase coherence and at best the sidelobe level will be reduced to S/G where G is the gain of the array. The above is summarised in table 1 showing that in general the substrate should have low ε_r and not be thin, thus highlighting the usefulness of foam-like substrates[6] which we have confirmed experimentally. Fuller details are given in the literature[6] and in our experience this design data is essential to enable a choice of substrate to be properly made.

If an antenna design is perfected at microwave frequencies there is likely to be a problem in scaling it down in size to correspond precisely to the thickness of one of the substrates currently available for millimetre wavelengths. Some iteration on a trial and error basis will remove this problem and has been used by the present authors. For instance much of our work has been done at 90 GHz on Duroid with h = 0.127mm which corresponds to h = 0.787mm at 14.5 GHz.

2.2 Other factors

Having scaled an antenna down in size for millimetre operations there are many other potential difficulties such as

- possible increased dissipation in the microstrip lines
- material and manufacturing tolerances and temperature effects
- connecting the microstrip antenna to the main equipment
- integrating the antenna with other circuits.

3

As previously stated it is the loss at millimetre wavelengths which is regarded by the antenna community at large as the main disadvantage and is consequently the main subject of this fundamental investigation into design principles. Tolerance, operational and temperature effects can be significant but their cause is generally self evident for a specific design requirement and improvements are likely to be obtained by work of a development nature. The problem of connecting the antenna to the equipment and the question of integration with circuitry has not appeared as a major issue hitherto but we show that it is of fundamental importance.

The correct choice of substrate and scaling down in size of a micro-strip antenna design for millimetre wave operation is clearly only the first step in the overall design process involving the above factors but it is an important step which in the past does not appear to have been adequately quantified.

3. LAUNCHER RADIATION LOSS AND ASSOCIATED PROBLEMS

Rectangular metal waveguides have found universal use at millimetre wavelengths despite the considerable research interest in low loss dielectric waveguides. This situation is unlikely to change in the near future and hence the use of microstrip in the antenna structure necessarily involves the implementation of a transition to launch the incident waveguide wave into the microstrip and vice versa for a receiving antenna. Some radiation loss seems inevitable and we refer to this as the launcher radiation loss. In contrast it is not difficult to obtain an acceptable reflection loss over the relatively narrow operational bandwidth at millimetres. The radiation loss rather than reflection loss is thus the main problem, creating unwanted sidelobes and cross-polarisation effects in arrays with critical specifications in these respects.

Some typical waveguide to microstrip launching transitions are shown in Fig 3 and a photograph of the backfed launcher is shown in Fig 4. Initially the backfed launcher[7] was thought to be the most useful for incorporation in our measurement benches but each launcher has disadvantages. A photograph of two E-plane launchers[8,9] in a measurement rig for line loss is shown in Fig 5. The ridge waveguide launcher[10] has been reported in circuit applications and did not appear to have any particular advantage over the above types so it was not examined. The triplate launcher[11] Fig 6a is useful at microwaves but would appear to be difficult to make accurately at millimetres due to the excessive relative thicknesses of conductor and substrate creating unwanted parallel plate modes in the triplate. The coaxial launcher[11] Fig 6b is somewhat similar to the backfed launcher being a probe but is only likely to be viable for short lengths of cable at millimetre and will again be difficult to assemble. Although the waveguide launcher will necessarily be mainly employed it is important to examine the likely radiation loss of all the above types as follows.

3.1 Estimates of launcher radiation loss

This is a mathematical problem of formidable difficulty and the measurement of the loss is equally difficult. The order of loss could be around 1% of the power supplied to the antenna which seems a small quantity at first sight and is commonly ignored when transitions are used in circuit applications. Such a fraction of uncontrolled radiation could limit sidelobe and cross polarisation levels to -20dB as a rough estimate and in this sense is very significant. Probably the only calculations[11,12] on this topic have been those of the RMCS research group and resulting estimates for the coaxial, triplate and backfed launchers are given in table 2 and Fig 7. The power losses are seen to be less than 1% for h/λ_o values typical of millimetre antennas, that is $h/\lambda_o \sim 0.05$. These three launchers can be regarded as aperture coupling devices whereby the field generated by the launcher needs to be as similar in nature as possible to the microstrip guided wave being launched to achieve low radiation loss. If the launcher field is $(\underline{E}_L, \underline{H}_L)$ and the microstrip field is $(\underline{E}_m, \underline{H}_m)$ then a measure of the similarity of the fields and hence the launching efficiency η is

5

$$\eta = \frac{1}{16 \ P_L P_m} \ |\int_A (\underset{\sim}{E}_m \times \underset{\sim}{H}_L - \underset{\sim}{E}_L \times \underset{\sim}{H}_m) \cdot \underset{\sim}{Z} \ da|^2 \qquad (1)$$

where P_L and P_m are the power flows in launcher and microstrip and
A is the launching aperture. The direction of the fields is $\underset{\sim}{Z}$ and
$-Z$ so that η tends to unity when the fields become similar.
This formula based on the Lorentz reciprocity theorem[44] or alternatively
reaction principles suggests a simple way of estimating the radiation
loss but the loss $(1 - \eta) \times 100\%$ includes both the reflected and radiated
power. Our more recent analysis[11] has been based on a more complete
variational process.

Obtaining estimates of radiation loss for the E plane and ridge
waveguide transitions Fig 3 presents additional analytical problems
because they are all of a 'choke-like' nature. That is their apertures
are designed to be cut-off waveguides to the incident waveguide mode
arriving at the opening while establishing the launching action by a
two-wire connection. That is a wire connection to the strip conductor
and another to the ground plane. However currents running over the end
faces of the waveguide opening give rise to radiation and no analytical
estimates are available to date. Some existing experimental data is
shown in Table 3.

When the launcher radiation loss is at a significant level it also
becomes a source of unwanted cross-polarisation[3]. To assess the latter
for aperture coupling devices it seems reasonable to compute the radiation
pattern corresponding to the incident field in the aperture and compare
the polarisation properties with that of the antenna. We have doubts
about the validity of this calculation because it takes no account of
the coupling process evident in eqn (1). Previous analytical results[14]
show that launcher radiation patterns can develop nulls in directions
where efficient wave transfer occurs thus supporting the doubts expressed
here. At the present time no analytical results for launcher cross-
polarisation can be recommended and we rely on inspection of the
measurements of the radiation patterns of the combined antenna and
launcher action.

3.2 Measurement of launcher loss

The E-plane launcher Figs 3 and 5 appeared to us to have been
well developed by others[8,9] for circuit operation and although its
radiation loss received no mention it seemed likely that it was fairly

well optimised in this respect. It was the first type that we investigated and outline measurement details are given in appendix 9.2. The E-plane launcher loss at microwave frequencies in Table 4 are not competitive with those of Fig 7 for aperture type launchers and at millimetres the E-plane launcher loss is at an even higher level which would be unacceptable in many applications. The error in measurement at millimetres is probably about 0.1dB but even so does not account for the large loss which after consideration we attribute to some increased dissipation loss in the transition and mechanical tolerances. The cross-polarisation from the launcher is significant and has been discussed in section 5. Many trial and error experiments were performed with lossy material inserts to locate the regions in the launcher responsible for both the high radiation loss and its polarised nature. Internal serrated chokes were used by the original developers[8,9] of this transition and the characteristics of such chokes described elsewhere.[15] However we could not establish the radiation role of any of these chokes which in any case were not practical propositions at millimetre wavelengths. In the end we found that much of the unwanted radiation was generated by the end faces of the waveguide where the incident waves experience the transition from a balanced closed transmission system to an unbalanced open one. Printed baluns were placed at the ground plane interface with no effect on the radiation although a beneficial tuning effect was evident in the reflection loss characteristic. We conclude that the original design[8,9] had been optimised without regard to radiation effects and no significant reduction in the latter could be brought about for this particular physical structure.

Our attention was next focussed on the backfed transition Figs 3 and 4 which seemed to be a simpler arrangement and had already been used in one antenna design by others.[7] The launcher loss at microwave frequencies Table 4, is somewhat better than the E-plane device and clearly operates over a much wider bandwidth. It was thought that this might be due to the relative simplicity of the arrangement whereby the backfed launcher was simply the tip of a coaxial cable entering the substrate from the ground plane side. At millimetres a backfed probe was waveguide mounted as in Fig 3 and a 3 stub tuner had to be included in the waveguide run. The construction of the tuner is noted in section 5.1 and the launcher losses Table 4 for the entire backfed probe/tuner assembly, are very high. We attribute this to the additional dissipative losses in the 3 stub tuner which are not untypical in matching devices having large internal standing waves. Several experiments were performed to reduce the size of conducting surfaces within the assembly in the hope of reducing dissipative losses but no significant improvements can be reported.

3.3 Summary of findings on launcher radiation loss mechanism

Several transitions have been built and tested at microwave and millimetres. Analytical estimates have been derived but only give the order of radiation power loss. Measurements confirm that high internal dissipative losses can exist within the launchers even if reflection loss is low. The internal losses can be reduced by careful design ensuring good internal matching but constructional/machining requirements are unrealistic at millimetres. The E-plane launcher has to date given best performance but cross polarisation problems still exist.

7

4. MICROSTRIP LINE LOSS

The dearth of information on losses in microstrip at millimetre wavelengths and somewhat confusing attitudes about the degree of loss, was evident in the literature study; a summary of salient points is given in appendix 9.3 and this information formed a good foundation for our subsequent investigations, confirming that little had previously been established about the actual line loss mechanisms.

A computer programme was compiled based on a collection of formulas from various sources. Dielectric and conduction losses were derived from the work of Schneider[16] and Pucel[17,18] respectively while roughness formulas were extracted from Hammerstad and Bekkedel[19] and Morgan[20]. At lower frequencies Pucel's formula may slightly over estimate the loss and the roughness formula strictly pertain to much lower frequencies. The computed results for constant h/λ_o ratios are in Fig 9 and extensive measurement at millimetres on a microstrip line using the method of appendix 9.2 are given in Fig 10a. A comparison of the computed and measured results shows that there is a factor of two to one difference or more depending on how the error tolerances on the measurements are interpreted. For instance at 90 GHz the average measured result is around $0.23dB/\lambda_m$ compared to the computed value of $0.1dB/\lambda_m$ (including roughness). In these measurements E-plane transitions and 5cm and 10cm lengths of specimen line were used. The insertion loss measurements were corrected for reflections at the input transition but frequent dismantling of the assembly was necessary as part of the calibration process and it is considered that this increased the scatter of the measured results. These results are in fact the first detailed evidence we have seen regarding the order of loss at millimetres. It must be emphasised that in this measurement that although the launcher loss is eliminated in the calculation the nature of the launchers may have a bearing on the result. The measurements were repeated using a backfed probe arrangement with launcher losses reported in Table 4 yet despite the high launcher loss the results of Fig 10b show less error scatter than those in Fig 10a and have a trend closely following the computed result. We believe the results of Fig 10b to be the more reliable.

Our conclusion is that the loss of microstrip at millimetre wavelengths is not excessive compared to microwave frequencies and computed results as in Fig 9 are a reasonable indication of the behaviour. The antenna problem therefore seems to amount to the fact that microstrip is too lossy at microwave frequencies and we need to seek innovative changes at the latter frequency in the first place. We now report on various studies to reduce microstrip loss without sacrificing the simplicity of the microstrip geometry and the low manufacturing costs.

4.1 Effect of preparation of copper conductor

As discussed in appendix 9.3 line losses can be reduced somewhat by paying attention to the question of surface roughness, choosing metal surfaces which are as smooth as possible. A commonly used dielectric

8

material is RT-DUROID made by the Rogers Corporation, USA. This glass
filled Teflon substrate comes with 1, ½ and ¼ ounce per square foot weights
in both electrodeposited and rolled copper. Recently polished copper
cladding has been added to the range. The surface roughness of electro-
deposited copper is about 30% of the total thickness while polished copper
has a surface roughness of about 1.5%. Fig 11 is a series of four electron
microscope photographs which show the surfaces of electrodeposited and
rolled copper in 1 and ¼ ounce weights. It is evident from the photographs
that although there is a visible difference in surface roughness between 1
and ¼ ounce electrodeposited copper there is little visible difference
between the two weights for rolled copper and the surface is very much
smoother.

To good approximation the roughness can be regarded as triangular
in nature as sketched in Fig 11 where the resulting Δ/δ values at 10 and
100 GHz are listed. When these are substituted into Morgan's equation
of appendix 9.3 it is immediately apparent that the line loss at millimetre
wavelength is not significantly reduced by the use of rolled rather
than electrodeposited copper but there is some improvement at 10 GHz. For
instance from the data in Fig 11 $\Delta/\delta = 3.79$ increases the line loss by
a factor ~ 2 whereas $\Delta/\delta = 0.64$ leads to an increase of only 1.4. The
inference here is somewhat surprising, suggesting that there is little
point in using other than electrodeposited copper at 90 GHz unless a
surface roughness significantly less than that of rolled copper can be
obtained. Some measurements on rolled copper at millimetres are shown in
Table 5 and confirm the above inference when a comparison is made with
the electrodeposited copper results of Fig 10b.

4.2 Feasibility of low permittivity substrates

At microwave frequencies the microstrip substrate is thick enough to
allow low permittivity foam substrates to be utilised without unduly
sacrificing structural strength and rigidity. The electrical advantages
gained by the use of these low density substrates has already been discussed
in section 2 and an obvious question is whether the concept can be extended
to millimetre wave bands. The likely advantage would be removal of the
dielectric loss and some reduction in the conductor loss due to the wider
strip creating a more even current distribution with relatively less current
flow along the strip edges; as discussed in appendix 9.3. The computed loss
Fig 12 supports these deductions as may be seen by comparison with the
curves of Fig 9. We have attempted to fabricate low permittivity substrates
of a foam composition but so far the substrate thickness has been of the
order of air bubble size and a dielectric skin, much as Mylar sheet, has
to be superimposed to allow deposition of the conducting strip. Such a
skin occupies a significant volume of the substrate region and complicates
the assembly. To date we are not able to recommend any technological
processes to enable the electrical advantages associated with the low
permittivity substrate concept to be realised.

4.3 Two-dimensional Litz wire concept

Litz wire[21] is composed of fine insulated strands of wire woven in such

a way that it acts destructively against the skin effect[22] in a wire used
at radio frequencies and thus reduces the losses. The idea is simply that
the peripheral current flows in each strand periodically thus forcing
the current flow away from the surface and distributing it more evenly
across the cross sections of the stranded structure. Litz wire does
not function at higher than broadcast radio frequencies but nevertheless
we have attempted to emulate the concept in two rather than three
dimensions. The microstrip line was serrated with oblique slots as in
Fig 13 and it was conjectured that the current flow along the strip edges
might be distributed more evenly over the surface helped perhaps by
capacitive coupling across the slots. If the slots caused the current
path length to increase then this would of course be counterproductive.
Several lines with differently arranged slots were tested but no significant
change in line loss was detected. Since periodic structures have stop and
pass bands we were not surprised to see this effect as shown in the insertion
loss curves of Fig 13 where the stop band commences at 14 GHz. This idea
was considered to have been sufficiently well examined at microwaves and
no experiments at millimetres were conducted. Maintaining the slot resolution
at millimetres would however have presented problems.

The possibility of using this concept to create integral antenna/
stop band filters is worthy of note but was not pursued.

4.4 Rounding of conductor edges

The idea here is to remove the sharp edges of the conducting strip
and hence distribute the current more evenly to reduce loss as discussed
in appendix 9.3. The first question that was addressed was the order of
improvement in losses that could be achieved and this was investigated
for a round airspaced wire above a ground plane Fig 14. The aim is to
compare the conductor loss α_{cw} of the wire structure with that of air-
spaced microstrip having the same impedance and separation from the ground
plane as sketched in Fig 14. Using the formulas of Wheeler, we obtain

$$\alpha_{cw} = \frac{(\pi f \mu / \sigma)^{\frac{1}{2}} \quad (\frac{1}{a} + \frac{1}{b})}{2\pi \sqrt{1 - (\frac{a}{b})^2} \quad 60 \cosh^{-1}(\frac{b}{a})} \quad \text{nepers/cm} \tag{2}$$

$$\mu = 4\pi \ 10^{-9} \ \text{henry/cm}$$

$$\sigma = 5.8 \times 10^5 \ \text{S/cm}$$

a and b are in cm

To compare with microstrip we take the two criteria of Fig 14 based on
either approximate equality of wire diameter or mean height. Some typical
results not including roughness correction are given in Table 6 and show
that the loss can only be reduced by about 50% at the expense of replacing
the planar strip with a much wider and bulkier round wire. We assume
that this order of loss reduction will be maintained when a substrate is

inserted but we are then faced with relinquishing the easy to print
planar advantages of the microstrip for a wire structure that requires
lateral support presumably by embedding it in the substrate. An alternative
is to try to build up and round off the edges of the microstrip line after
printing to perhaps achieve some degree of loss reduction without
sacrificing the simplicity of manufacture.

It was found that if a microstrip structure is subjected to electro-
plating to greatly increase the copper thickness, noticeable rounding of the
edges occurs. Surface pitting and edge fissures become more pronounced in
the plated lines and are likely to negate any loss reduction arising from the
rounding of edges. Details of a series of experiments are shown in Fig 15
and the best results that have been obtained are given in Table 7; these
are seen to be a small improvement. Our conclusion is that although the
improvement is small the technique leaves the main cost/planar advantages
of microstrip geometry virtually unaltered.

4.5 Summary of techniques for reducing microstrip line loss

The line loss of microstrip increases at millimetres to about $0.13 dB/\lambda_m$
at 90 GHz compared to about $0.1 dB/\lambda_m$ at 20 GHz. The increase is less
than generally assumed and there is a need to reduce the loss pedestal
at microwave. Four ideas have been investigated and the outcome is thus:

a. Copper conductors need a degree of surface smoothness, beyond
that obtainable commercially at present, to effect a noticeable
reduction in loss.

b. Low permittivity substrates would reduce losses but are impractical
at millimetres.

c. Serrating the conducting strip to make current flow more uniform
has had little or no effect on losses.

d. Heavy electroplating rounds off strip edges giving some small
reduction in loss. The use of round wires is impractical at milli-
metres but would give a reduction in loss.

The conclusion is that either heavy electroplating or some technique
for creating very smooth copper surfaces can give some small reduction
in line loss (about $0.02 dB/\lambda_m$). It seems unlikely that these two techniques
could be used together.

11

5. TYPICAL STATE-OF-THE-ART SYSTEM LOSSES FOR MILLIMETRE MICROSTRIP ANTENNAS

The loss mechanisms investigated above will now be considered with respect to typical microstrip antennas, prior to summarising the state-of-the-art on system loss factors. Some of the many special components that have been manufactured by us to facilitate measurement are mentioned. Travelling wave comb linear arrays using E-plane and backfed probe launchers are involved and parallel fed patch arrays are also included.

5.1 Linear comb antenna

A 30-finger comb linear array was designed using our computer manufacturing facility. This travelling wave antenna was designed to have a broadside beam at 15.5 GHz so that when scaled down by the ratio of available substrate thicknesses of 6.2:1, would operate near to 90 GHz. An E-plane launcher was fitted to both the microwave and millimetre versions of the antennas as shown in Fig 16. The radiation patterns at microwave are shown in Fig 17; the high level of cross-polarisation is due to the E-plane launcher and has been mentioned in section 3.2; the reduction in cross polarisation is evident when a coaxial launcher is used and this is shown in Fig 17. The power budgets for the antennas are given in Table 8 and using this data it follows that at 90 GHz the microstrip line loss is 0.14 dB/λ_m which compares very well with the measurements of Fig 10b. The computed gain in Table 8 is based on $4\pi A/\lambda_o^2$ where A = the aperture area and the power dumped in the terminal is measured at 2.63 dB. It is seen that the efficiency at 90 GHz is about 5% worse than at 15.5 GHz and is assumed to be due to the increased feeder line loss at millimetres. It is considered that errors due to the use of the simple gain function are common to both antennas and therefore do not affect the accuracy of the comparison.

To test the overplating technique another comb antenna was produced and made thick by electroplating as described in section 4.4. The above gain budgets were measured at 90 GHz and a slightly improved efficiency indicated a reduction in line loss of 0.03 dB/λ_m which is compatible with the value obtained in Table 7.

A millimetre antenna pattern measurement rig was constructed to enable the antenna and launcher to be rotated in a controlled manner. A typical radiation pattern is shown in Fig 18 but the apparatus was not sensitive enough to show much of the sidelobe structure or the cross-polar radiation. There is no evidence at hand to suggest that the patterns are very different from those in Fig 17.

At one stage in the research it was anticipated that the backfed probe launcher would be superior to the E-plane launcher but as already discussed in section 3.2 this is certainly not so at millimetres. The high loss has been attributed to internal losses in the 3-stub tuners, mechanical details of which are shown in Fig 19. The theoretical

radiation loss from a backfed launcher has been shown in Fig 7 and is very small compared to the measured losses of Table 4. We believe that with further development the internal losses of the backfed probe and tuner assemblies could be reduced but the E-plane launcher remains at present the easier of the two to design and manufacture.

5.2 Parallel fed patches

The microstrip patch antenna is now becoming commonplace at micro-wave but feeder effects in large arrays of patches create significant loss effects. A summary of measured results by others is given in Fig 20 to illustrate this point. To check the degree of loss in the patches Q measurements on a single millimetre patch at 78.6 GHz were performed as shown in Table 9. The approximate formulas[29] used are also listed and a typical reflection loss measurement Fig 21 enables the Q_T the total patch Q to be measured[30]. The patch efficiency is seen to be high confirming that feeders in large patch arrays are the main source of loss. It should therefore be possible to estimate the total loss due to T-junctions and bends in the feeder system and straight sections of lines. This is done in Table 10 and is seen to be a good model for estimating large arrays of patch antennas. This information can be presented as in Fig 22, to show that there is an optimum array size beyond which the gain decreases. As may be expected the feeder losses and hence gain are a function of spacing between the patches and this is illustrated in Fig 22.

5.3 State-of-the-art system loss in microstrip antennas

The most significant aspect of the measurements on microstrip line loss is that they provide substantial evidence that the loss is not much larger at millimetres than at microwave frequencies. Attitudes that we have previously experienced presume that microstrip becomes excessively lossy at millimetres and this is definitely not so. The precise value of loss depends on the microstrip dimensions but for system comparisons here it is sufficiently accurate to state that losses for 50Ω lines of the following order are to be expected.

$$\sim 0.1 \quad dB/\lambda_m \text{ at 20 GHz}$$
$$\sim 0.13 \text{ } dB/\lambda_m \text{ at 90 GHz}$$

This information is based on our measured results and agrees reasonably well with the computations provided surface roughness is included. From our experiments on ways of reducing loss in section 4 it is probably feasible to reduce the 90 GHz loss to 0.11 using overplating (section 4.4) and ultra low loss substrate with ε_r as low as possible.

5.3.1 Travelling wave and resonant linear arrays at 90 GHz

Our data on transitions and line loss enables the system loss diagram of Fig 23 to be compiled. It is assumed that the travelling wave

array has a transmission line N_λ microstrip wavelengths long but apart from this its precise form is unspecified. The assumption here is that any type of microstrip linear travelling wave array[31] will be comprised of a microstrip feeder to which microstrip elements are attached or embedded within the feeder. The dominant loss will be that of the feeder which is $\ell_g = N_\lambda \alpha$ where α = loss dB/microstrip wavelength. The other losses are the launcher transition loss ℓ_ℓ, a small loss due to the element dissipative loss and the loss in the terminal load ℓ_t; the latter two quantities are not included in Fig 23. Since conventional waveguide is predominantly used in present-day millimetre equipment we assume that the launcher transition is of the waveguide to microstrip type and we have taken a launcher loss of 0.3-0.4dB depending on the degree of field 'binding' in the microstrip line. Such a loss could be typical of E-plane and ridge waveguide launchers and includes both radiation and dissipative losses internal to the launcher structure. Our reference to field 'binding' in the microstrip is explained as follows. For circuit operation the microstrip fields must be tightly bound to the structure to minimise radiation[32] at discontinuities and ξ must be made large where

$$\xi = \frac{Z_m \, \epsilon_e}{640} \left(\frac{\lambda_o}{\pi h}\right)^2$$

Z_m is the microstrip line impedance and ϵ_e the effective relative dielectric constant. For antenna applications the field needs to be loosely bound and ξ small which implies a thicker substrate but to prevent excessive surface wave generation

$$\frac{h}{\lambda_o} < \frac{1}{4(\epsilon_r)^{\frac{1}{2}}}$$

The computed line loss of microstrip lines having three different types of substrate for both antenna and circuit applications is as given in Fig 23.

This diagram presents the state-of-the-art for linear travelling wave arrays and can be used as follows. A 20 wavelength long array on a substrate $\epsilon_r = 2.32$ has a principal system loss of about 2.3dB to which must be added the power lost in the line terminal load (possibly 0.3dB) and a similar amount due to the loss in each radiating element. The total loss would then be 2.3 + .3 + .3 = 2.9dB. The element loss is approximately the loss in one element since the elements are all fed in parallel across the line. If a tightly bound microstrip structure had been used the line loss contribution would have been about 4dB higher due to the binding of the field to the ground plane and strip conductor. The important issue here is that integration of the antenna with microstrip circuitry is a possibility whereby the launcher loss of 0.4dB would be removed but the line loss would increase by 4dB making a total antenna loss of 2.3 + 4 + .3dB = 6.6dB.

With a linear resonant array[33] there is a standing wave on the microstrip feeder brought about by removing the terminal load. Resonant arrays are very narrow band but simpler in that there is no terminal load. In the above example the loss of 2.3 + .3 + .3 = 2.9dB would seemingly be reduced to 2.6dB but in reality the loss would increase due to the resonator action[34] of the feeder as experienced previously by us. The precise loss is very much a function of the particular resonant structure and no more general information can be extracted.

Finally aperture gain data is presented in Fig 24 for the conditions of Fig 23 and clearly shows the limitations due to line losses. The small reduction in line loss by the techniques of section 4 will have little effect on the situation.

5.3.2 Parallel fed patch arrays

We now extend the gain assessments of section 5.2 to produce design aids. Measurements are also shown based on arrays such as the example in Fig 25. In Fig 26 the array gain is estimated under the conditions stated and compared with measured arrays. The intrinsic patch element loss plays a smaller part in the loss mechanism and radiation from corners and bends is the dominant effect. Our calculation assumes that these latter losses are phase incoherent and do not create radiation in the main beam. The relative loss effects are quantified in Table 10. A limiting gain of about 27dB corresponding to a 32 x 32 array and 5% efficiency is evident. The calculations are repeated at millimetres Fig 27 and show only slightly reduced gain. The calculation includes radiation losses at corners and bends based on the microwave estimates in Table 10. Launcher loss has not been included in Fig 26 and 27.

These curves are useful state-of-the-art guidelines for this type of array and will also give a good indication of the array loss budget when other than square patches are used.

5.3.3 Implications for military applications

Comparison of Fig 24 with Fig 27 show that square arrays of linear arrays for ϵ_r = 2.3, have a limiting gain of about 36dB compared to 27dB for square patch arrays. This is due to the greater feeder lengths in the patch system. However the linear system requires a corporate feed thus incuring additional loss and probably equalising the loss with that of the patch system. Where they differ is in sidelobe and cross-polarisation with the patch array becoming more difficult to control for larger array sizes. The linear array however needs to be many wavelengths long to enable the power to radiate out along the length. This all points to the conclusion that patch antenna arrays are more suitable for low gains and linear arrays for higher gains. It now remains to identify antenna applications in relation to antenna size and permissible losses and a summary is given in Table 11. While generalisations seldom give really sharp indications there is much evidence to suggest that submunition

15

applications with their highly constrained space are ideally suited for microstrip patch antennas and small arrays of the latter. The linear array does not fit in well with any of the applications because its gain maximum is below the limit demanded. This does not mean that use of linear arrays is to be abandoned because there will be many special applications to the contrary but we expect the general trend to be as previously stated. Exceptions to this will be when a low cost conformal planar structure is vital.

6. THE HYBRID DIELECTRIC/MICROSTRIP ANTENNA AS A COMPROMISE DESIGN TO REDUCE FEEDER LOSS

The present research has established that no significant reduction in microstrip line loss can be expected and on long linear arrays or arrays containing a multiplicity of microstrip feeder lines, a large dissipation loss will be incurred. To good approximation this is the summation of the individual losses of all series feeders and is generally unacceptably high for many applications. It now remains to investigate any compromise situation where some increased manufacturing complexity might be permissible if a worthwhile reduction in antenna loss were obtained and it is obvious that it is the microstrip feeder lines and not the individual microstrip radiating elements, where attention needs to be focussed. It is well known that dielectric open waveguides[35] have very low loss and compounding all the above facts we have converged on the new concept of the hybrid dielectric/microstrip antenna. Simply stated the concept is to replace long microstrip feeders with very low loss dielectric lines but retain the printed assembly of radiating elements. This leads us to the choice of insular guide[36] whereby a rectangular dielectric slab line is attached to a dielectric substrate backed by a ground plane; the intention being to design the substrate to suit microstrip antenna requirements (section 2) and dimension the dielectric slab for efficient waveguide action. We will not concern ourselves with ways of utilising the insular guide as an antenna by creating discontinuities in it (i.e. steps or metal scatterers) because our studies[37] show that such radiators do not give pattern control comparable to that obtained with microstrip antennas.

The investigation of the hybrid antenna concept thus centres around devising ways of coupling the microstrip elements to the dielectric guide. The main question is then the reduction in antenna loss obtainable. Pattern control, purity of polarisation and manufacturing complexity are some of the other factors that may be equally important in some applications.

6.1 Coupling to narrow matched microstrip lines

It has been previously established[38] that wire radiators can be embedded into round dielectric rods in a controlled manner and more recently similar results have been demonstrated[39] for insular guide where the wire elements were in proximity. Our approach is illustrated in Fig 28 where a microstrip line lies normal to the insular guide. The line is a distance x_o from the axis of the dielectric slab of width 2C and may be isolated $(x_o > C)$ or protrude underneath $(x_o < C)$. Patents[40,41] dealing with antenna and circuit applications exploiting the hybrid concept have been taken under the restricted condition of higher mode operation in the dielectric guide. In this section we describe the coupling to a matched narrow microstrip line and show the behaviour for different modes in the dielectric guide. The first step is to calculate the phase constant β for the modes of interest in the dielectric guide and we use

17

the simple but approximate effective dielectric constant method.[42,43] Some results are shown in Fig 29.

The coupling of dielectric and microstrip structures is calculated using the Lorentz reciprocity theorem.[44] The percentage of insular guide power P_I coupled to the microstrip line is

$$100 \frac{hw}{P_I} \left(\frac{\varepsilon_{r1} \varepsilon_o}{\mu_o}\right)^{\frac{1}{2}} \frac{\left|\int_A \underset{\sim}{E}_I \cdot \underset{\sim}{E}_M \, dA\right|^2}{\left|\int_A \underset{\sim}{E}_M \cdot \underset{\sim}{E}_M \, dA\right|^2} \%$$

where $(\underset{\sim}{E}_I, \underset{\sim}{H}_I)$ and $(\underset{\sim}{E}_M, \underset{\sim}{H}_M)$ are the fields in the dielectric guide and microstrip line respectively and h, w and ε_{r1} are defined in Fig 28. This formula does not account for radiation and reflection in the region where both guides physically interact and is further approximated by the assumption of TEM field forms for $(\underset{\sim}{E}_M, \underset{\sim}{H}_M)$ and the simple field forms $(\underset{\sim}{E}_I, \underset{\sim}{H}_I)$ arising from the effective dielectric constant method. The coupling aperture A is the rectangular cross-section of the microstrip line underneath the conducting strip of area hw in the plane of the insular guide dielectric/air boundary. Computed results Fig 30 show the way coupling varies with distance x_o and the disparity in coupling values either side of $x_o = C$ is due to the approximate field forms for (E_I, H_I). The effect of strip width w is shown in Fig 31 and the oscillatory nature is due to the axial periodic nature of the dielectric line fields.

6.2 Hybrid antenna using narrow microstrip lines

The coupling results Figs 30 and 31 suggest that a travelling wave antenna can be constructed by deploying microstrip lines along the insular guide, each line having an appropriate x_o value to ensure that the power flowing in the lines, when radiated, creates a desired aperture distribution along the antenna length. The simplest way of radiating the power is to terminate the lines in an open circuit and for tuning purposes the length of line together with end corrections and other evanescent effects is made one half wavelength long. Finally the separation between the lines is dictated by the phase constant β, the desired mode and desired direction of the beam.

Experiments[45] on antenna arrays designed as above indicated that the E_{21}^x mode coupled better than the E_{11}^y mode contrary to Figs 30 and 31; patterns for arrays using the E_{21}^x mode at both microwave and millimetres are shown in Fig 32. At microwave the launching transition was a coaxial connector attached to a short length of 1mm wide microstrip line 15mm long; cross polarisation levels were < 15dB and the sidelobe level was consistent with the choice of x_o = constant for each microstrip stub. While the antenna itself was very efficient with the only significant power loss being that of the terminating load in the travelling wave case, the antenna system loss was around 5dB due to the radiation loss

18

of the launcher. Radiation patterns for the millimetre antennas were corrupted by additional radiation losses from the launcher which was simply an open-ended waveguide containing the insular guide offset to one side.

This higher-order hybrid array has achieved the aim in that a linear antenna with very low feeder loss has been devised but there are serious drawbacks. First, launching to the higher mode is a problem and unless lower launcher losses are possible, the overall antenna system loss is worse then for a comparable microstrip array. Second, it is very undesirable to deploy microstrip lines beneath the dielectric slab from a manufacturing standpoint; air spaces or ill-defined thicknesses of adhesive create large variations in β and hence affect the antenna phasing. A third point concerns the actual physical action and it would appear that the E_{21}^x mode enables more power to be extracted from the insular guide than the E_{11}^y mode due to a high degree of scattering that is not embraced in the results of Figs 30 and 31. Another possible problem with working the E_{21}^x mode is the likelihood of mode conversion to the E_{11}^y at discontinuities and generation of low level unwanted radiation.

6.3 Coupling to rectangular microstrip patch resonators

In this investigation we set out to restrict operation to the E_{11}^y mode and microstrip not protruding under the dielectric guide. It was evident that coupling levels would be lower and the use of wide microstrip stubs was suggested, ultimately leading to deployment of microstrip patch resonators along the dielectric line. It was also decided to calculate β and the insular guide fields as accurately as possible and a mode matching method, similar to that used for image guide was evolved[46]; computed results for β are shown in Fig 29 for comparison. The accuracy of the fields is greatly improved but some disparity still remains in the field values at the dielectric boundaries.

The microstrip patch has width w as in Fig 28, but with finite length ℓ in the x direction and $x_o > C$; a modal expansion of the patch fields is formulated where for example

$$E_{yp} = \sum_{p=1}^{\infty} \sum_{q=1}^{\infty} \frac{B_{pq}}{\varepsilon_{r1} k_o^2 - k_{pq}^2} \cos\left(\frac{p\pi z}{w}\right) \cos\left(\frac{q\pi (x - x_o)}{\ell}\right)$$

where p and q are integers and the resonance condition is given by

$$\varepsilon_{r1} k^2 - k_{pq}^2 = 0$$

$$k_{pq}^2 = \left(\frac{p\pi}{w}\right)^2 + \left(\frac{q\pi}{\ell}\right)^2$$

19

Computed resonances for $p = 1$, $q = 0$ and $p = q = 1$ modes are compared in Fig 33 with measurements at 8.5 GHz; the disparity in w illustrating sensitivity to material and dimensional tolerances.

Loss mechanisms in the resonator are represented by Q-factors Q_c, Q_d and Q_r denoting conductor, dielectric and radiation losses respectively. These losses are embraced in this analysis as an effective bulk dielectric loss in the resonator by invoking an effective loss tangent

$$\tan \delta_e = \frac{1}{Q_r} + \frac{1}{Q_c} + \frac{1}{Q_d}$$

hence the coefficients B_{pq} can be calculated once the excitation apertures are identified. The latter are taken on two end faces of the rectangular microstrip patch i.e. in the planes $x = x_o$ and $Z = 0$. The magnetic field in each aperture due to the insular guide fields is related to a fictitious current source which in turn defines the patch field coefficients B_{pq}. A Fourier decomposition is used in this process. Since radiation is the dominant effect the coupling is expressed as the percentage of insular guide power that is radiated by the microstrip patch and computed results are given in Fig 34. Measured results Fig 35 showing the total power loss confirm the general behaviour with w and ℓ changes and the disparity in actual w values illustrates tolerance sensitivity in the experimental model. A practical patch width of about 11mm corresponds to half wavelength $(\lambda_m/2)$ resonator action and it is seen that higher coupling results when $\ell = \lambda_m/4$ rather than $\lambda_m/2$.

The variation of coupling with x_o is shown in Fig 36 and there is considerable disagreement between the order of the computed and measured results. We consider the measurements to be less reliable because the only way of connecting instruments to the insular guide to proceed with the method of section 9.2, was to use horn-type launchers which can feasibly couple direct to the microstrip patch. However the general order of coupling portrayed by Fig 36 establishes that the E_{11}^y mode can be coupled to microstrip patches without making direct contact and at a level that permits a linear array to be constructed.

6.4 Hybrid antenna coupling E_{11}^y mode to microstrip patch resonators

Details of the above design procedure are illustrated in Figs 37 and 38 where the stubs are microstrip resonators with $w = \lambda_m/2$ and $\ell \sim \lambda_m/4$. The x_o distances are calculated from Fig 36 to give a uniform aperture distribution and to date the empirical curve gives the best radiation pattern. However the radiation leaking from the guide load is very pronounced and insufficient power has been coupled to the resonators showing that a more precise coupling relationship must be achieved to get control of the design. This must be compounded with the need for tighter physical tolerances in the substrate and bonding of guide to the latter. The squint away from broadside is such a tolerance effect. The feeder loss, Table 12 is much less than for a microstrip linear array of comparable aperture size and establishes the principle but launcher radiation is the remaining problem which negates the latter.

20

7. CONCLUSIONS AND RECOMMENDATIONS

7.1 Conclusions

a. The design problems associated with microstrip antennas at microwaves have been identified (section 2) and dissipative losses and manufacturing tolerance effects can be expected to worsen at millimetre wavelengths. Of these, dissipative losses are considered to be the major obstacle requiring attention.

b. This investigation has established that the increase in microstrip line loss with frequency is not as great as the concensus of opinion has hitherto suggested (section 4 and 5.3).

c. The connection of the microstrip antenna to the receive and/or transmit equipment is a major laboratory measurement and operational problem that has generally been underestimated in the literature (section 3). Large increases in antenna system loss and radiation pattern corruption (increased sidelobe and cross polarisation) can occur if the launching transitions are not optimised. This is a field compatibility problem and ideally the microstrip antenna needs to be fed by microstrip circuitry but even then some problems exist (section 5.3.1). Several types of launching transitions have been investigated (section 3). At microwaves launcher performance, acceptable for some applications, has been demonstrated (section 3.2) and the coaxial type is generally superior to waveguide launchers. At millimetres the performance of launchers has been degraded mainly by the physical difficulty of making precision measurements during development and subsequent problems in precision machining of such small waveguide assemblies. Loss mechanisms in launching transitions have no doubt in the past obscurred the precise behaviour of microstrip antennas at millimetres which may have led experimenters to deduce that it is the microstrip itself which has become excessively lossy.

d. An extensive investigation (section 4) into ways of reducing the microstrip line loss both at microwave and millimetres has established that little can be done if the manufacturing and operational advantages of the microstrip structure are to be retained. The effect of copper surface roughness, dielectric substrate material and the conducting strip geometry have been investigated (sections 4.1 to 4.4). A surprise result is that surface roughness must be reduced many orders to have any noticeable effect at millimetres.

e. Gain curves and system power budgets for arrays of linear and patch microstrip antennas have been compiled based on our latest loss and other data (section 5). The constraints on achievable system gain and other performance factors enable the implications for military applications to be deduced (section 5.3.3).

21

Microstrip patch arrays are seen to be well suited to applications
such as submunitions where space is limited, gains need not be
high and conformal low cost assemblies are demanded.

f. The hybrid antenna concept (section 6) has been evolved to
eliminate feeder loss while retaining many of the desirable
features of the printed assembly. The concept itself has been
demonstrated but launcher losses at present negate the inherent
advantages. This is again a field compatibility problem and this
type of antenna is ideally suited to integration with insular
guide circuits at such times as the latter have reached an
acceptable level of development. Mechanical and constructional
tolerances are more difficult to control because the dielectric
guide has to be bonded to the substrate. The optimisation of
the aperture distribution also depends critically on the precise
interaction between resonators and dielectric guide. Second order
'end effects' due to evanescent fields contribute to the exact
behaviour and further development work is required. The stacking
side-by-side of linear arrays to create a two dimensional array is
a possibility.

7.2 Recommendations

a. The fundamental performance of microstrip antennas at milli-
metre wavelengths is in principle identical with operation at
microwaves apart from a moderate increase in loss. This conclusion
assumes that dimensions can be accurately scaled down, tolerances
held and homogeniety of materials maintained. The following
approach to millimetre microstrip antenna design is thus recommended.

    1. Inspect microwave microstrip antenna performance data
and allowing for some increase in line loss, ascertain
whether, when scaled in frequency, it would satisfy the
millimetre specification.

    2. If the answer to 1. is positive then assess the
feasibility and cost of scaling down dimensions while
maintaining tolerances etc. Even if micro-machining and
fabrication methods are cost effective relative to the
project aim the substrate specification may not be met by
commercially available products.

    3. An important aspect of scaling is that if a sufficiently
accurate translation is carried out fewer measurements are
necessary at millimetres thus cutting test costs.

22

b. Although there is little prospect of achieving substantial
reductions in microstrip line loss there is much pure fundamental
research to be done in quantifying the various effects contributing
to the mechanism.

c. The hybrid antenna is an interesting new concept and worthy of
further development, particularly with respect to the launching
problem. . The possibility of creating very large millimetre arrays
is challenging in that it would require a compatible corporate feed.

d. .The connection of the microstrip antenna to its receiver and/
or transmitter is seen as a fundamental physical compatibility
problem of considerable difficulty. As such greater emphasis should
be given to the concept of integrated antenna receiver (or trans-
mitter) assemblies where in principle launching transitions do
not arise.

e. Evidence has been cited[37] that other ways of creating planar
arrays at millimetres are also problematical and in this light
microstrip may yet be the best structure to use. It is recommended
that the state-of-the-art comparison of microstrip and other
antennas at millimetres be made clear to assist system designers
achieve a balanced viewpoint and endorse the design approach
stated in item 7.2a. above.

8. REFERENCES

(1) J.R. James, P.S. Hall and C. Wood: 'Microstrip antenna theory and design', IEE(UK) Electromagnetic Wave Series 12, (Peter Peregrinus Ltd, London and New York) 1981.

(2) I.J. Bahl and Bhartia: 'Microstrip antennas', (Artech House, 1980).

(3) P.S. Hall and J.R. James: 'Cross polarisation sources in comb line microstrip antenna arrays', 3rd IEE International Conference on Antennas and Propagation, Norwich, 1983, pp 454-458.

(4) R.T. Davis: 'Millimeter-waves: controversy brews over transmission media', Microwaves, March 1976, pp 32-42.

(5) Communication to J.R. James from Lt Col J.F. Harvey US Army ERO, 10th Feb 1982 (and enclosures from RADC US Airforce).

(6) J.R. James, A. Henderson and P.S. Hall: 'Microstrip antenna performance is determined by substrate constraints', Microwave Systems News, Aug 1982 pp 73-84.

(7) M.A. Weiss: 'Microstrip antennas for millimetre waves', Ball Brothers Report ECOM-76-0119-F, Oct 1977.

(8) J.H.C. Van-Heuven: 'A new integrated waveguide to microstrip transition', IEEE Trans, MTT-24, March 1976, pp 144-147.

(9) L.J. Lavedan: 'Design of waveguide-to-microstrip transitions specially suited to millimetre-wave applications', Electron Lett (GB), Vol 13, No 20, Sept 1977, pp 604-605.

(10) P.M. Brigginshaw and J.E. Curran: 'Study of microstrip circulators and isocirculators in the frequency band 65-95 GHz', GEC Hirst Labs Report No 16,682C for DCVD research project RP4-128.

(11) A. Henderson and J.R. James: 'Design of microstrip antenna feeds, Part 1, Estimation of radiation loss and design implications', Proc IEE (UK), H, 128, 1981, pp 19-25.

(12) P.S. Hall and J.R. James: 'Design of microstrip antenna feeds, Part 2, Design and performance limitations of triplate corporate feeds', Proc IEE (UK), H, 128, 1981, pp 26-34.

(13) J. Arnold and R.S. Butlin: 'Extended frequency range GaAs MESFETs using 0.3m gate lengths', Proc 11th European Microwave Conference, Amsterdam, Sept 1981, pp 264-269.

(14) J.R. James and A. Henderson: 'High frequency behaviour of microstrip open-circuit terminations', Microwaves, Optics and Acoustics, Vol 3, No 5, Sept 1979, p 210.

(15) K. Tomiyasu and J.J. Bolus: 'Characteristics of a new serrated choke', IRE Trans, MTT-4, Jan 1956, pp 33-36.

(16) M.V. Schneider: 'Dielectric loss in integrated microwave circuits', Bell System Tech Jour, Sept 1969, pp 2325-2332.

(17) R.A. Pucel: 'Loss in microstrip', IEEE Trans, MTT-16, No 6, June 1968, pp 342-350.

(18) R.A. Pucel et al: 'Correction to Losses in Microstrip', IEEE Trans MTT-16, 1968, p 1064.

(19) E.O. Hammerstad and F. Bekkadal: 'Microstrip Handbook', ELAB Report STF 44 A74169, University of Trondheim, Norwegian Institute of Technology, 1975.

(20) S.P. Morgan: 'Effect of surface roughness on eddy-current losses at microwave frequencies', J App Phys, 1949, 20, pp 352-358.

(21) F.E. Terman: 'Radio Engineers Handbook', (McGraw-Hill New York, 1950) p 37.

(22) (a) H.A. Wheeler: 'Formulas for skin effect', Proc IRE 30, pp 412-424.

(b) H.A. Wheeler: 'Transmission line properties of a round wire in a polygon shield', IEEE MTT-27, No 8, 1979, pp 717-721.

(23) J.H.C. Van Heuven: 'Conduction and radiation losses in microstrip', IEEE Trans MTT-22, Sept 1974, pp 841-844.

(24) H.M. Barlow: 'High frequency impedance of a practical metal surface and the effect of a thin coating of dielectric over it', Electron Lett (UK), Vol 6, No 13, June 1970, pp 413-415.

(25) F.J. Tischer: 'Excess conduction losses at millimetre wavelengths', IEEE Trans, MTT-24, No 11, Nov 1976, pp 853-858.

(26) F.J. Tischer: 'Experimental attenuation of rectangular waveguides at millimetre wavelenghts', IEEE Trans, MTT-27, No 1, Jan 1979, pp 31-37.

(27) G.E.H. Reuter and E.H. Sondheimer: 'The theory of anomalous skin effect in metals', Proc Royal Soc, Vol 195, 1949, pp 336-364.

(28) A.E. Sanderson: 'Effect of surface roughness on the TEM mode', Advances in Microwaves, (Academic Press), 7, 1971, pp 2-56.

(29) A. Gopinath: 'Maximum Q-factor of microstrip resonators', IEEE Trans MTT-29, 2, 1981, pp 128-131.

(30) E.L. Ginzton: 'Microwave Measurements', International series on pure and applied physics, pp 413-417. McGraw-Hill book company, 1957.

(31) Reference (1) Chap 5.

(32) Reference (14) p 215.

(33) Reference (1) Chap 5.

(34) J.R. James and P.S. Hall: 'Microstrip antennas and arrays Pt 2 - new design technique', IEE Jour on Microwaves, Optics and Acoustics, 1, 1977, pp 175-181.

(35) T. Itoh: 'Dielectric millimetre wave integrated circuits', Chap 5 in Infra-red and Millimetre Waves, Vol 4, Millimetre Systems, Ed K.J. Button and J.C. Wiltse, Academic Press 1981.

(36) R.M. Knox: 'Dielectric waveguide microwave integrated circuits - an overview', IEEE Trans, MTT-24, 1976, pp 806-814.

(37) A. Henderson and J.R. James: 'A survey of millimetre wavelength planar antenna arrays for military applications', Rad and Electronic Eng, 52, Nov/Dec 1982, pp 543-550.

(38) R.H. Duhamel and J.W. Duncan: 'Launching efficiency of wires and slots for a dielectric rod waveguide', IRE Trans, MTT, July 1958, pp 277-284.

(39) M.R. Inggs et al: 'Experimental 30 GHz printed array with low loss insular guide feeder', Electron Lett, Vol 17, No 3, 1981, pp 146-147.

(40) On antenna arrays European Patent Number 82 302702.4, 1982.

(41) On image guide circuits, British Patent Number 8303597.

(42) P.P. Toulios and R.M. Knox: 'Image line integrated circuits for system applications at millimetre wavelengths', Final Rep Contract DAAB07-73-C-0217, US Army Electronics Command Report ECOM-73-0217-F, July 1974.

(43) R. Mittra et al: 'Analysis of open dielectric waveguides using mode matching technique and variational methods', IEEE Trans MTT-28, 1980, pp 36-43.

(44) H.M. Barlow and J. Brown: 'Radio surface waves', (Oxford Univ Press 1962) pp 82-87.

(45) A. Henderson, E. England and J.R. James: 'New low loss millimetre-wave hybrid microstrip antenna array', Proc 11th European Microwave Conference, Amsterdam, Sept 1981, pp 825-830.

(46) K. Solbach and I. Wolff: 'The electromagnetic fields and the phase constants of dielectric image lines', IEEE Trans MTT-26, 1978, pp 266-274.

(47) M.A. Weiss: 'Microstrip antennas for millimetre waves', IEEE Trans AP-29, No 1, pp 171-174, January 1981.

(48) J.C. Williams: 'A 36 GHz printed planar array', Electron Lett (GB), Vol 14, No 5, pp 136-137, 2nd March 1978.

9. APPENDICES

9.1 Administrative and other details

Mr Chris Hall was appointed a research scientist on this contract in February 1982.

Learned contributions during this project period by Professor James and members of the RMCS group specifically relating to the millimetre wave band are as follows:

   i. In September 1981 (with co-authors A Henderson and E England) presented a paper on a 'New low loss millimetre wave hybrid micro-strip antenna array' at the European Microwave Conference, Amsterdam.

   ii. In February 1982 organised an IEE colloquium in London on 'Advances in the design and manufacture of microstrip antennas'. With co-authors A Henderson and P S Hall, he read a paper on how to choose a substrate for optimum operation.

   iii. In March 1982 (with co-authors G John and A Henderson) a paper was presented on 'Some aspects of millimetre wave antennas' at the 8th Queen Mary College Symposium on Antennas, London.

   iv. 'Microstrip antenna performance is determined by substrate constraints'. Published in Microwave Systems News, August 83, by James, Henderson and Hall.

   v. In September 1982 (with co-authors G John and A Henderson) a paper was presented on 'Analysis of insular guide launcher radiation and comparison with microstrip counterparts', at the European Microwave conference, Helsinki.

   vi. In October 1982 (with co-author A Henderson) a paper was presented on 'A critical review of millimetre planar arrays for military applications' at the Military Microwave conference, London. A fuller account was subsequently published as reference 35.

   vii. Professor James and Professor Douglas Harris (University of Wales) are guest editors of a special edition of the IERE Radio and Electronics Engineer Journal (November/December issue) on 'Millimetre wave systems'.

9.2 Measurement of line and transition losses

The basic layout is sketched in Fig A4. Power measurements were made using a Hughes thermistor power head and a Hewlett-Packard 432A power meter. The directional couplers had a coupling level of -10dB and directivity of -40dB. Microstrip line loss measurements were made using two separate lengths of transmission line and two transitions of the same type which were, for practical purposes, assumed to be identical. Power levels were measured directly in milliwatts at locations A and B in the diagram. The following power levels were measured.

P_r = power reflected from a short circuit placed at Z_1.

P_t = power reaching load when the flanges at Z_1 and Z_2 are directly connected.

P_r' = power reflected from the line between Z_1 and Z_2.

P_t' = power reaching load when the line is placed between Z_1 and Z_2.

The % power loss in the specimen line thus equals

$$\left(1 - \frac{P_r'}{P_r} - \frac{P_t'}{P_t}\right) \ 100\%$$

When the specimen line requires launching transitions either end then the loss of these is included with the line loss. Details are

T = loss (dB) in launcher

L_2 = loss (dB) in longer line of length l_2

L_1 = loss (dB) in shorter line of length l_1

T_2 = total loss (dB) of two transitions plus longer line loss

T_1 = total loss (dB) of two transitions plus shorter line loss

$$l_2 = nl_1 \text{ and hence } nL_1 = L_2 \text{ where } n > 1$$

$$T_1 = 2T + L_1, \quad T_2 = 2T + L_2$$

$$T_2 - T_1 = L_2 - L_1 = (n - 1) \ L_1$$

Therefore $T = \dfrac{nT_1 - T_2}{2 \ (n - 1)}$ dB.

L_1 and L_2 can then be calculated and hence the line loss. In our experiments $n = 2$.

9.3 Physical effects creating line loss

The subject of dissipative losses in microstrip antennas has not been comprehensively tackled even at low microwave frequencies probably because accurate measurements of loss and its associated mechanisms are difficult. Much past work on losses has been directed towards microwave integrated circuits built on alumina substrates and because of its empirical nature is of little use at millimetres.

The first published work specifically about microstrip losses was written by Pucel[17]. Much of the work was fundamental in nature but included measurements on Rutile substrates showing a steady rise in loss up to 6 GHz. Pucel stated, "...... in a microstrip line over a low dielectric constant substrate the predominant source of microwave loss at microwave frequencies are the non-perfect conductors". 'Non-perfection' includes the fact that the high frequency currents concentrate in the surface of a conductor[22] giving an increasing conductor resistivity with frequency. It also includes the effect of conductor roughness[20] and the effect of the rectangular cross-section of the conductor. The early work on rectangular strip conductors at high frequencies shows that the increase in resistance of the conductor is not due to the non-uniformity of the current within the strip but the crowding of current at the edges. Fig A1 shows the general form of the current density distribution $J_1(x)$ and $J_2(x)$ around a microstrip line. Current density increases towards the edge of the strip and if the strip were to become infinitely thin the edge current density would become unbounded which means the loss would be infinite. It is now obvious that the conductor loss or "ohmic attenuation factor" would be lowered if the radius of curvature at the edges of the microstrip line could be increased or if the surface current density could be evened out around the whole perimeter of the line by some means, in which case the attenuation constant[17] α_c is minimised.

$$\alpha_c = \frac{R_{s1}}{2Z_m} \int_c \frac{|J_1|^2 \, dx}{|I|^2} + \frac{R_{s2}}{2Z_o} \int_{-\infty}^{+\infty} \frac{|J_2|^2 \, dx}{|I|^2}$$

Z_m = characteristic impedance of the microstrip.

$R_{s1,2}$ = $(\pi f \mu / \sigma)^{\frac{1}{2}}$, surface skin resistivity in ohms per square unit for line and ground plane respectively.

$J_1(x)$, $J_2(x)$ = the corresponding surface current densities for the line and ground plane respectively. (Contour C is around strip cross section.)

$|I|$ = magnitude of the total current per conductor.

The non-uniformity of the current density around the line makes α_c almost impossible to calculate exactly because of the complexity of these currents and the extreme difficulty in measuring them.

The surface roughness of the conductor is another important source of loss. The surface (or Eddy) currents, when flowing over a rough surface, follow the contours of the surface so a current sheet flowing over a rough surface covers more area than if it were flowing over a perfectly smooth surface, depending on the roughness. Morgan[20] suggested that the increase in eddy current loss is proportional to the additional surface area introduced by the walls of grooves in a rough surface providing that the depths of the grooves are of the same order as the skin depth. The skin depth $\delta = 1/(R_s \sigma)$ where R_s is defined above and σ = conductivity of the surface. He calculated that the effect of grooves transverse to the surface current flow is about three times greater than for longitudinal grooves. Fig A2 shows the effect of surface roughness upon power dissipation relative to a perfectly smooth surface where the increased attenuation constant α_{CR} is given by[19]

$$\alpha_{CR} = \alpha_c \left[1 + \frac{2}{\pi} \tan^{-1} 1.4 \left(\frac{\Delta}{\delta} \right)^2 \right]$$

where Δ = RMS roughness of the surface. Inspection of this equation indicates that $\alpha_c \leq \alpha_{CR} \leq 2\alpha_c$. Curves of skin depth for various conductivities are given in Fig A3.

Van-Heuven[23] investigated the loss of shielded, open ended line resonators on quartz substrates for various surface roughnesses and found a good comparison with Morgan's results as shown in Fig A2. Barlow[24] suggested that any rough surface has, in conjunction with a resistive component of surface reactance, a capacitive component at high frequencies. Narrow crevasses in the path of current flow can introduce a capacitive component that dominates the behaviour of the surface if the crevasses are considerably greater in size than the skin depth of currents. He suggested that a thin layer of high dielectric constant material over a rough surface would reduce both resistive and capacitive components of surface reactance thus reducing the losses. It is not clear how much effect this would have upon a real microstrip line because most of the current flows in under surface of the conductor. An experiment was devised to test this but no benefits were observed.

Discrepancies have been measured between theoretical and measured surface resistance values for waveguide resonators, firstly in the 1 to 20 GHz region and then in the 20 to 300 GHz region[25,26]; also increases in the surface resistance of between 50 and 100% have been measured at 35 and 70 GHz. This effect is peculiar to copper at room temperatures (20 to 30°C) and is termed the 'room temperature anomaly of the skin effect'. It is separate from surface roughness and is, in part, responsible for the large discrepancies between theoretical and measured losses at millimetre wavelengths. The anomaly in the microwave region is a manifestation of an effect that has been observed in the infra-red and optical regions and is linked to the microscopic behaviour in the Noble metals Cu, Ag, Au, Su, Hg and Al. This subject merits further investigation[27] but is something that the practical engineer has to live with and find other means of reducing losses. The value of understanding the anomalous loss effect lies in being able to separate it from surface roughness effects

31

when interpreting loss measurements. We have not been able to make a distinction so far in our microstrip loss measurements.

Tischer described the increase in skin resistance in terms of an 'R$_s$ ratio' which is the ratio of the skin resistances of rough and smooth surfaces. He concluded that an anomalous skin effect in copper exists at room temperatures and that it may be described by an R$_s$-ratio of about 1.135. For a smooth surface work hardening increases the ratio to about 1.18 and that for rough surfaces where the surface roughness is much greater than the skin depth, the increase in the skin loss assumes a value proportional to the increase in surface area. A very detailed investigation of the effect of roughness on TEM wave propagation has been done by Sanderson[28] and provides additional useful data.

To date no information is available on line radiation at millimetre wavelengths generated by roughness. Rough conductor surfaces and edges would also act as scattering surfaces generating substrate surface waves and hence additional scattered radiation. This effect could have increased significance at millimetres. In conclusion our literature study has revealed mechanisms that may contribute to microstrip loss but their relative significance has not been quantified.
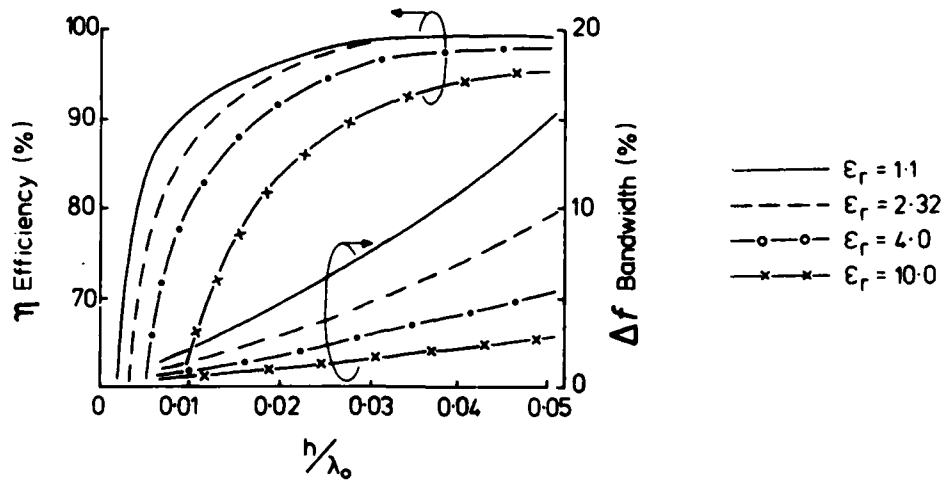
Fig 1: Relationship between bandwidth, efficiency and substrate
parameters.
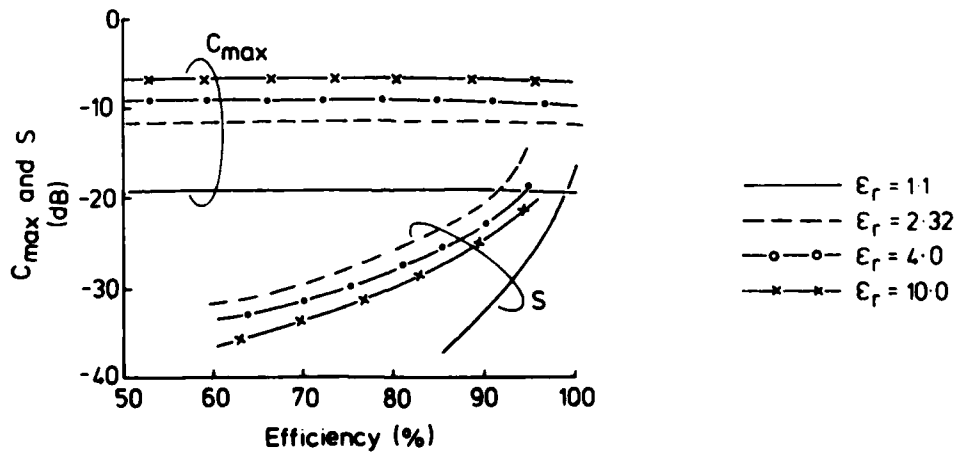
Fig 2: Relationship between efficiency, worst sidelobe level (S) and
cross polarization C_{max}.

33

SUBSTRATE	PERFORMANCE FACTORS				
	BANDWIDTH EFFICIENCY	X - POLAR	TOLERANCES	SIDELOBES (Surface-Waves) $\varepsilon_r<1\cdot8$	SIDELOBES (Surface-Waves) $\varepsilon_r>1\cdot8$
h	←	/	←	→	→
ε_r	→	→	→	→	←

← Increase to improve performance.

→ Decrease to improve performance.

Table 1: Summary of substrate parameters and their effect on antenna performance.

RIDGE.

E-PLANE.
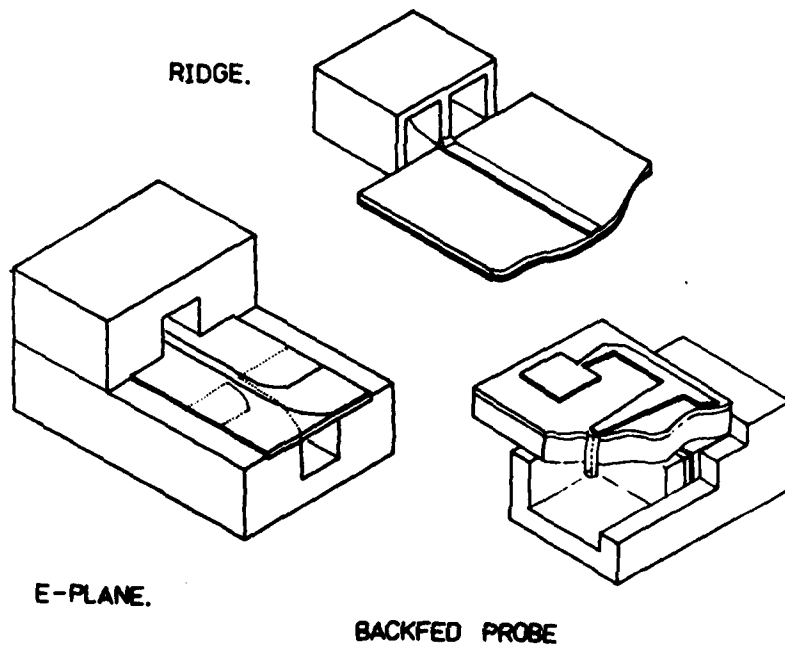
BACKFED PROBE

Fig 3: Pictorial view of waveguide to microstrip launching transitions.

Fig 4: Photograph of backfed probe launcher.
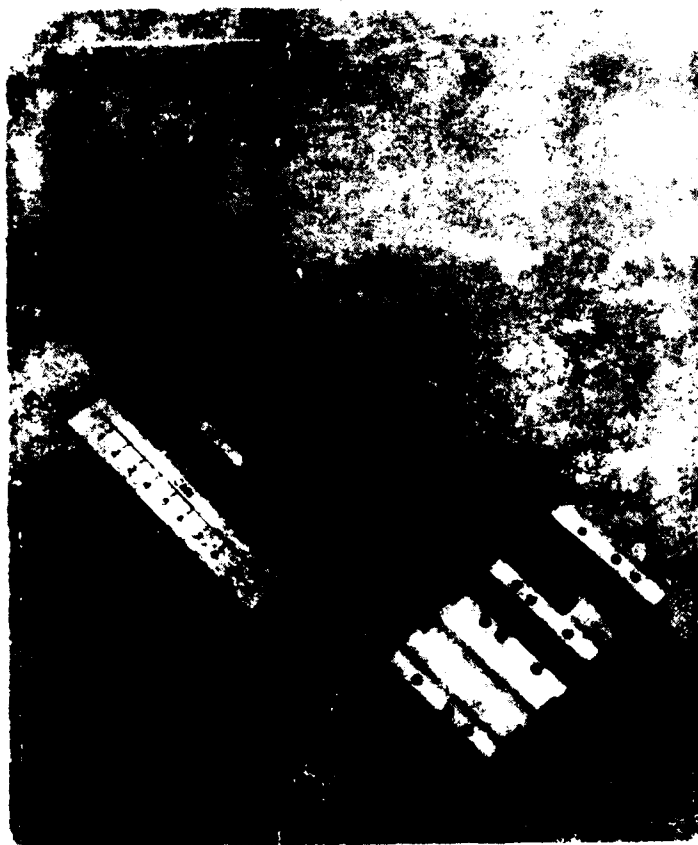
Fig 5: Photograph of E-plane launcher measurement rig.
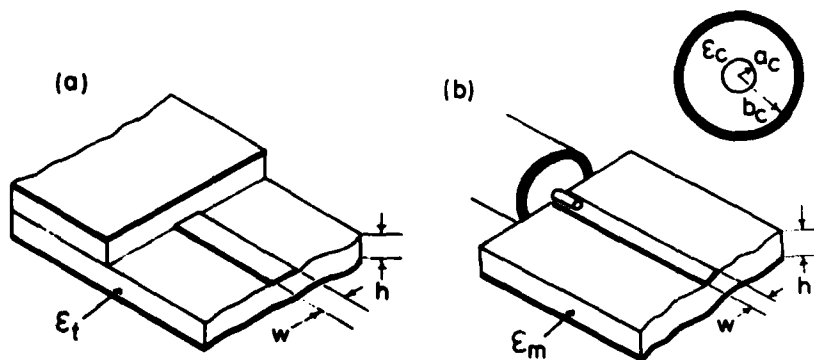
Fig 6: (a) Triplate to microstrip launcher,
(b) Coaxial to microstrip launcher.

Triplate Launcher

$$G_r Z_t \approx \frac{2\pi}{3} \frac{h}{\lambda_o} W_{et} \frac{1}{\sqrt{\varepsilon_t}} \quad (\times 100\%)$$

Coaxial In-Line Launcher

$$G_r Z_c \approx \frac{4}{9} (b_c - a_c)^2 a_c^2 \frac{Z_m}{\lambda_o^2 h^2} \quad (\times 100\%)$$

Matched Coaxial Probe.

$$\frac{1}{G_r Z_m} \approx \frac{60}{Z_m} \left[\frac{2\pi h}{\lambda_o}\right]^2 \left[1 - \frac{(\varepsilon_r - 1)}{2\sqrt{\varepsilon_r}} \log_e \frac{\sqrt{\varepsilon_r} + 1}{\sqrt{\varepsilon_r} - 1}\right] (\times 100\%)$$

G_r = Radiation Conductance.

Z_t, Z_c, Z_m = Impedance of Triplate, Coaxial and Microstrip Transmission Lines.

W_{et} = Effective Triplate Strip Width.

$a_c(b_c)$ = Inner (Outer) Radius of Coaxial Transmission Line.

Table 2: Formulas for launcher radiation loss.

Backfed Probe   Coaxial In-Line   Triplate
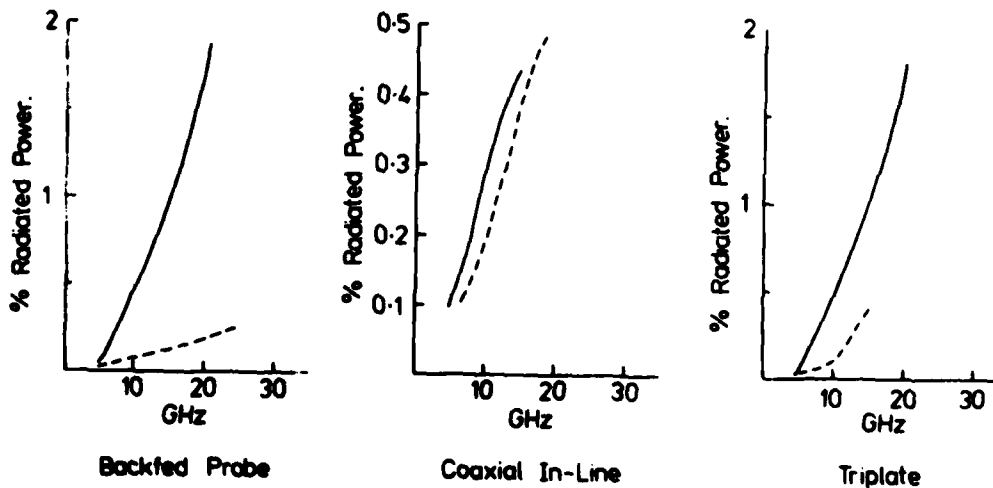
Fig 7: Radiation power loss as a percentage of antenna input power at the launcher.

	Polyguide	Alumina
ε_c	2·1	2·1
ε_m	2·32	10·0
a_c	0·64	0·45
b_c	2·07	1·48
h	0·79	0·50
Line Impedances		50 Ω

mm

37

Transition Details	Launcher	GHz	ϵ_r	Launcher Dimensions and Other Details	Launcher Loss dB (%)	
					Theory (radiation only)	Measured
waveguide to microstrip (ref 13)	Ridge Waveguide	40	4		—	0.25 (5.5)
waveguide to microstrip (ref 10)	Ridge Waveguide	85	2.3	Contact made using gold loaded epoxy	—	0.9 (19)
waveguide to microstrip (ref 10)	Ridge Waveguide	100	2.3	Contact made using gold loaded epoxy	—	1.0 (21)
Coax to microstrip (ref 11)	Coaxial Conductor	13	2.3	$h = 0.035\lambda_o$ 50Ω line. * Dominated by measurement error	0.0174 (0.4)	0.1* (2.5)

Table 3: Waveguide (ridge) and coaxial to microstrip, launcher loss comparisons

Freq (GHz)	Transition Loss (dB)		Scaled Freq (GHz) ×6·2	Transition Loss (dB)	
	E-Plane	Backfed		E-Plane	Backfed
12·00	——	-0·22	74·40	——	-5·4
12·25	——	——	75·95	——	-4·0
12·50	——	——	77·50	——	-3·6
12·75	——	——	79·05	——	-5·0
13·00	——	-0·42	80·60	-1·9	-5·9
13·25	——	——	82·15	-1·6	-6·1
13·50	——	——	83·70	-1·8	-6·8
13·75	——	——	85·25	-1·6	-7·4
14·00	——	-0·58	86·80	-1·6	-7·5
14·25	-2·30	——	88·35	——	-6·6
14·50	-0·34	——	89·90	-1·95	-6·1
14·75	-0·95	——	91·45	-1·90	-6·0
15·00	-0·48	-0·86	93·00	-1·98	-6·9
15·25	-0·56	——	94·55	-2·0	-6·1
15·50	-0·47	——	96·10	-2·0	-6·9
15·75	-1·70	——	97·65	-2·0	——
16·00	——	-0·64	99·20	-1·8	-8·6

Table 4: Transition loss of E-plane and backfed launchers at microwaves and millimetres (See Fig 8 for conversion to %).
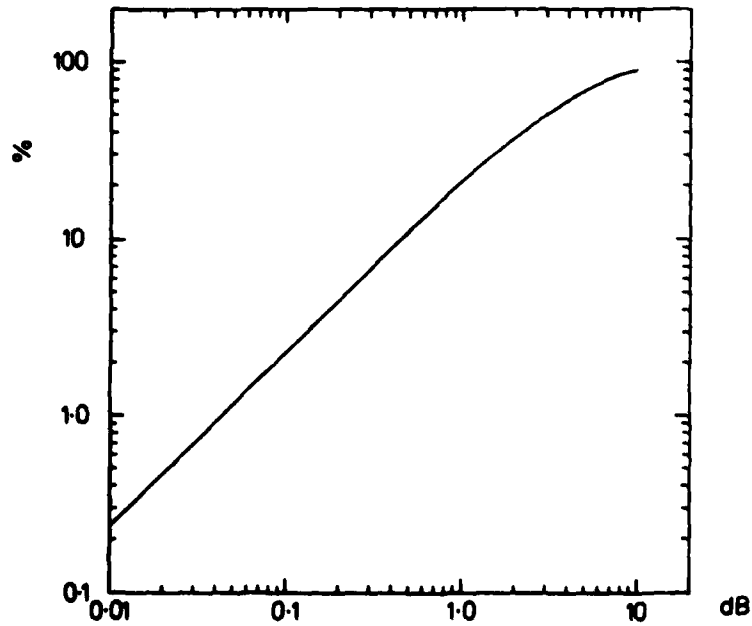
Fig 8: Conversion from dB loss to % loss.

(a) $\epsilon_1 = 2.32$ $\tan \delta = 0.001$
(b) $\epsilon_2 = 10.0$ $\Delta = 0.005$

- - - Dielectric Loss

-x-x- Conductor Loss (without roughness)

——— Conductor Loss (with roughness)

-·-·- Total Loss (with roughness)
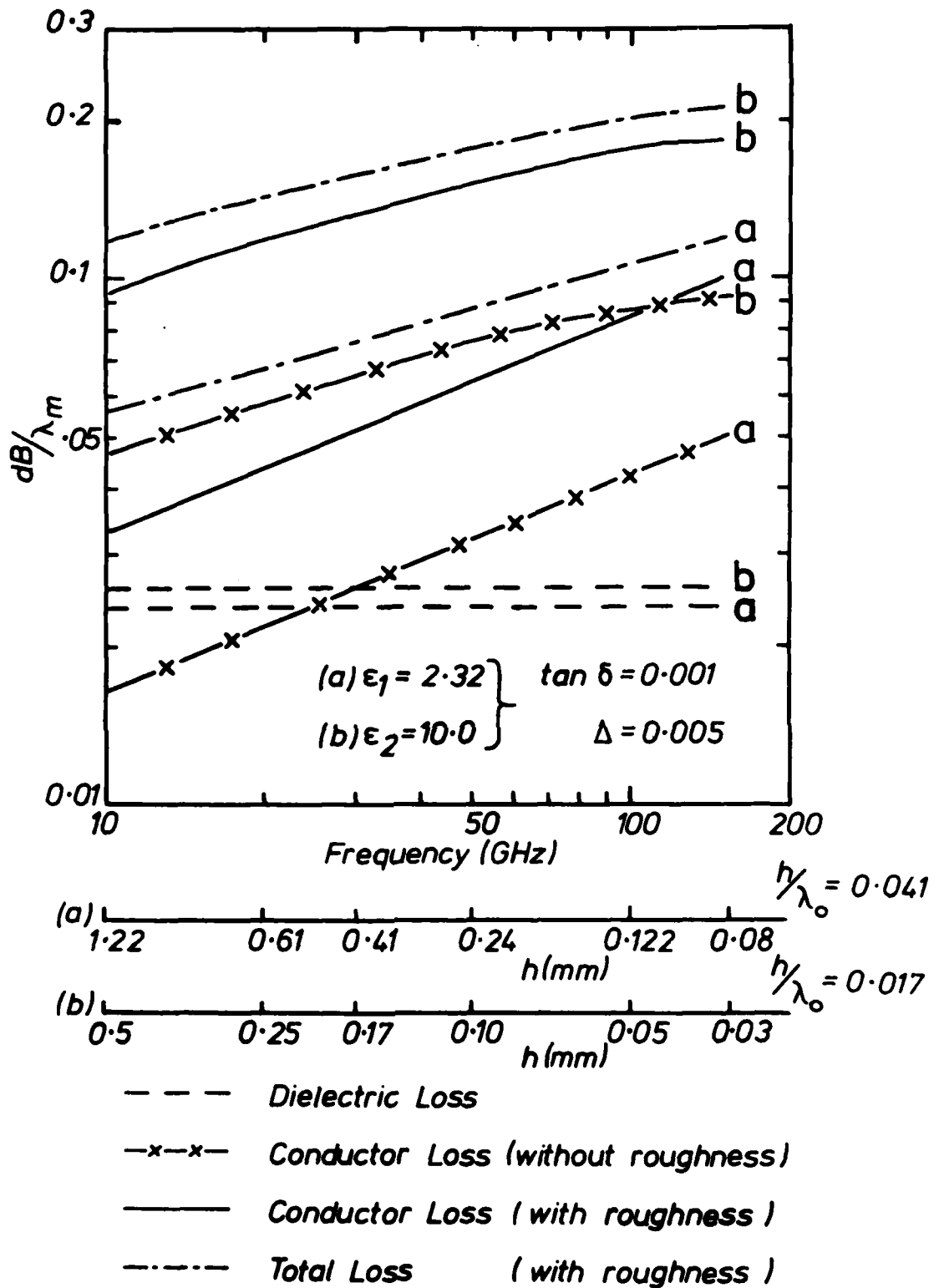
Fig 9: Computed microstrip (50Ω) line losses.
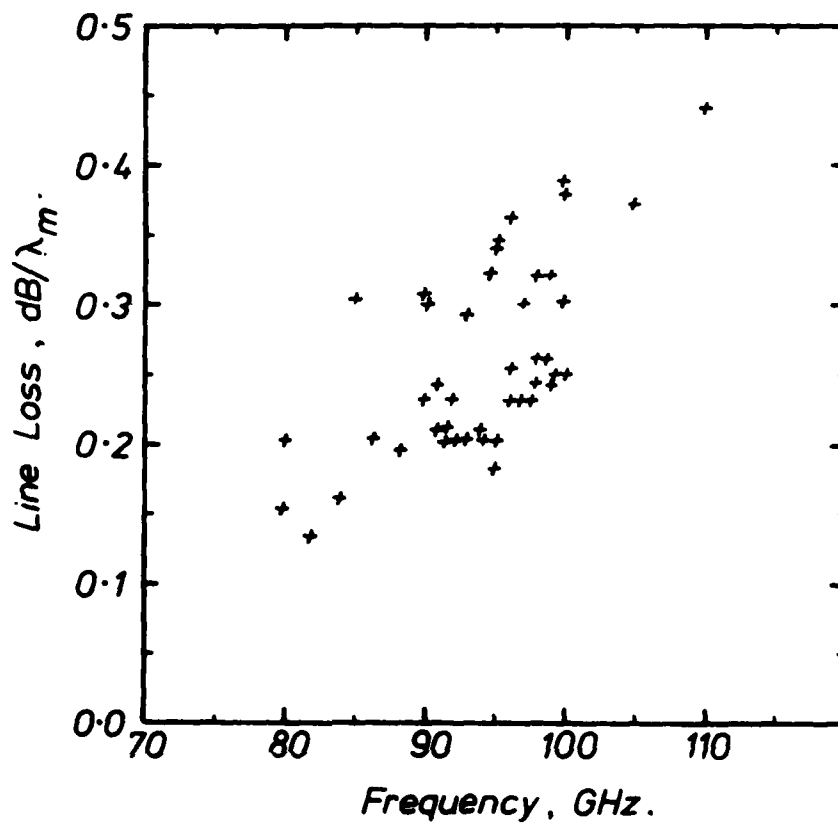
Fig 10(a): Microstrip line loss, theory and measurements using 5870
RT-DUROID clad with ¼ ozs electrodeposited copper and
E-plane launchers.
$\epsilon_r = 2.3$, w = 0.32 mm, h = 0.127, $Z_m = 50\Omega$.

41
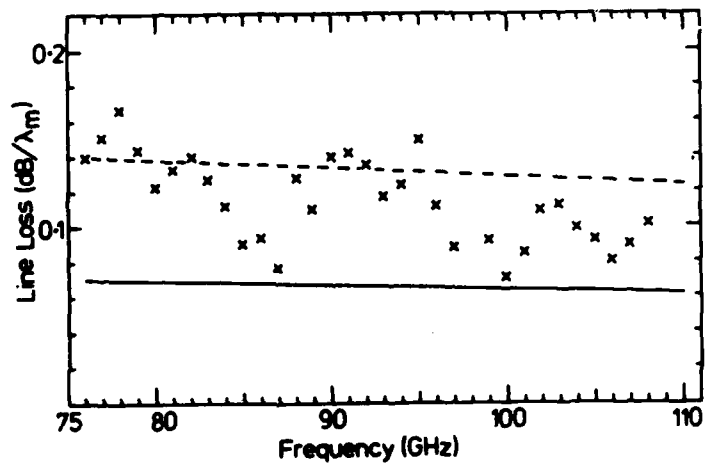
Fig 10(b): Microstrip (50Ω) line loss measurements, using backfed probe
launchers, on 5870 RT-DUROID clad with ½ ozs electrodeposited
copper.
ε_r = 2.3, w = 0.32 mm, h = 0.127 mm

42

(a)

$10\mu m$

$\Delta = 2\cdot5\mu m$

$100\ GHz$, $\Delta/\delta = 11\cdot96$

$10\ GHz$, $\Delta/\delta = 3\cdot79$

(b)

$5\mu m$

$\Delta = 1\cdot25\mu m$

$100\ GHz$, $\Delta/\delta = 5\cdot98$

$10\ GHz$, $\Delta/\delta = 1\cdot89$

(c)

$1\cdot7\mu m$

$\Delta = 0\cdot42\mu m$

$100\ GHz$, $\Delta/\delta = 2\cdot01$

$10\ GHz$, $\Delta/\delta = 0\cdot64$

(d)
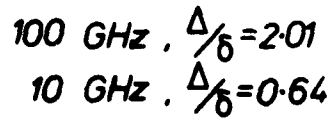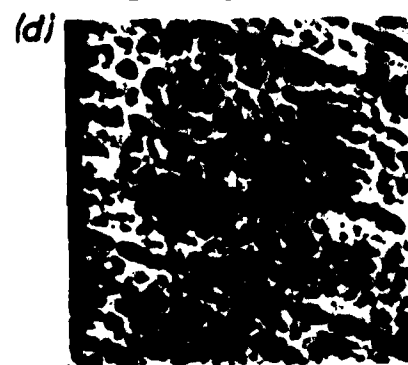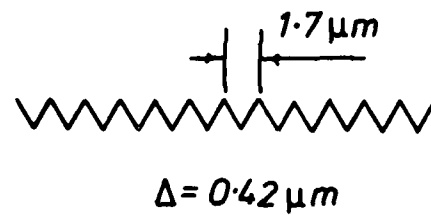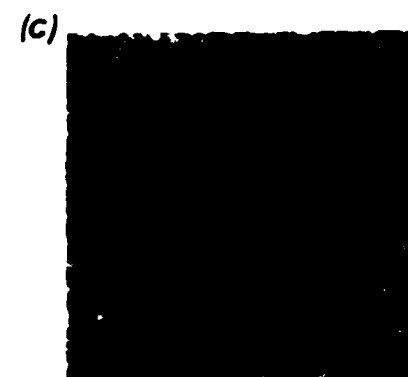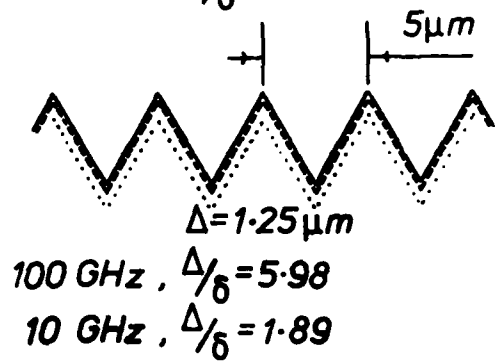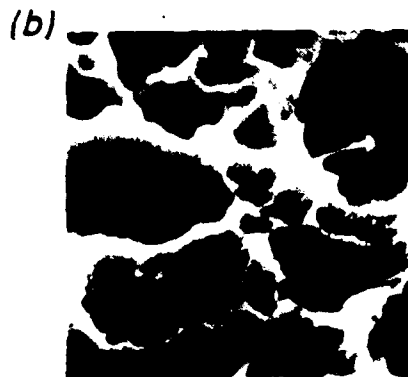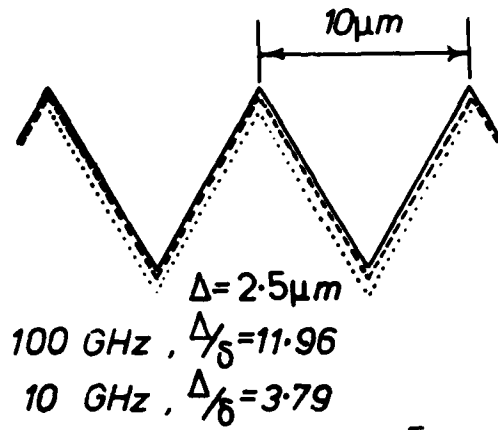
$100\ GHz, \delta = 0\cdot209\mu m$. $10\ GHz, \delta = 0\cdot66\mu m$.

(a), 1ozs Electrodeposited Copper.
(b)¹/₂ ozs   "   "
(c), 1ozs Rolled Copper.
(d)¹/₂ ozs   "   "

Fig 11: Surface roughness estimates from SEM photographs of etched 5880 RT-DUROID surfaces. Scale x 3000.

43
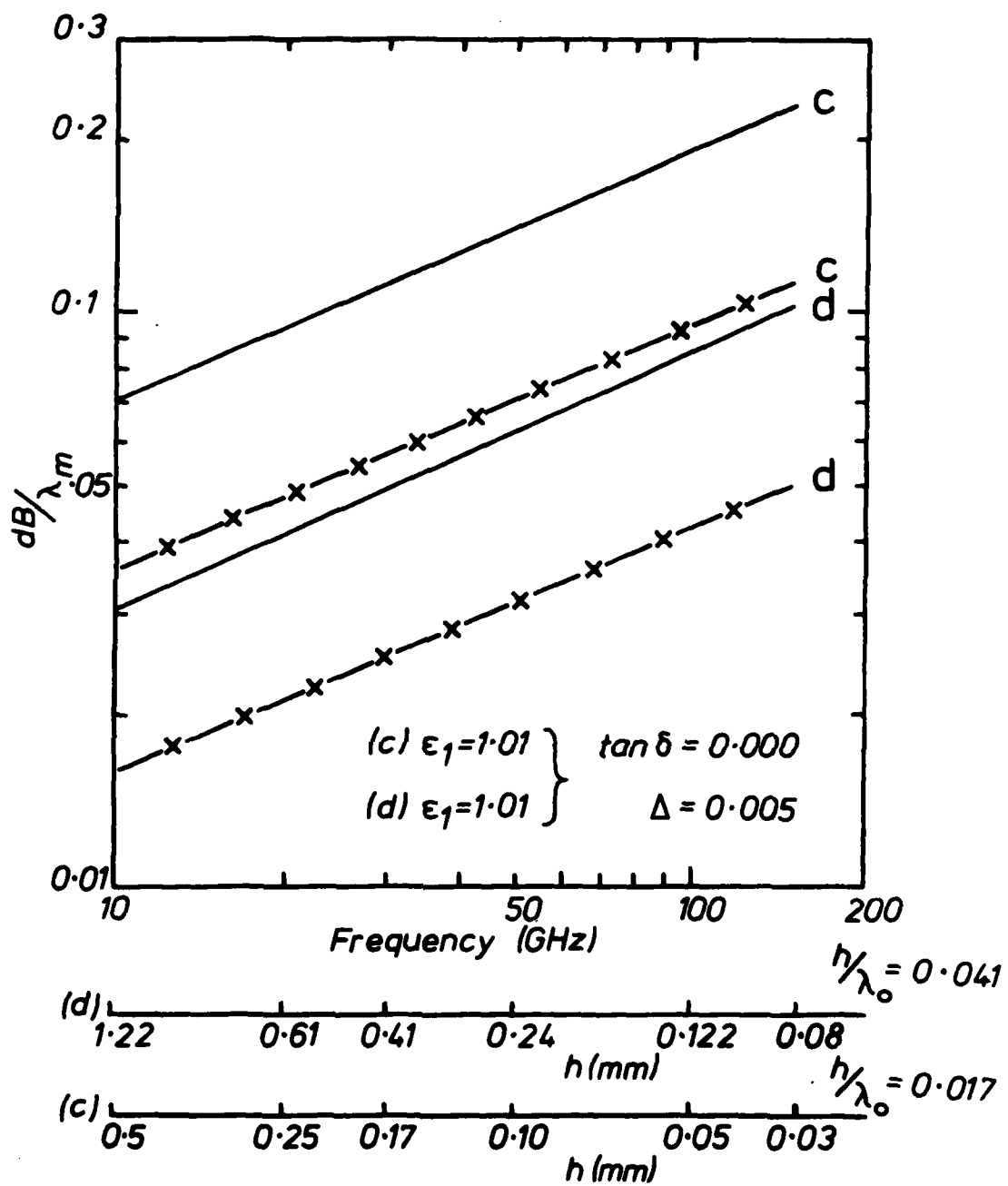
Fig 12: Computed microstrip (50Ω) line loss with foam substrates.

Material	Duroid 5870	Duroid 5880
ε_r	2.3	2.2
h(mm)	0.127	0.127
Copper Cladding	½ ozs electro-deposited	½ ozs rolled
Frequency (GHz)	78.6	79.8
Resonator size (mm)	1.02 x 1.02	1.02 x 1.02
ε_{eff}	2.2	2.1
Assumed line loss dB/λm	0.14	0.14
Q_o (calculated)	195.0	192.5
Q_R (calculated)	24.3	23.2
Q_T (calculated)	21.6	20.7
*EFFICIENCY (%) calculated	88.9	89.2
Q_T (measured)	43.7	40.9
*Q_R	56.3	51.9
*EFFICIENCY (%)	77.6	78.8

*Radiating efficiency $\simeq Q_T/Q_R$ x 100%

*Q_R inferred from measured Q_T and calculated Q_o values

Table 5: Efficiency comparison at millimetres between resonators made from Electrodeposited and Rolled copper
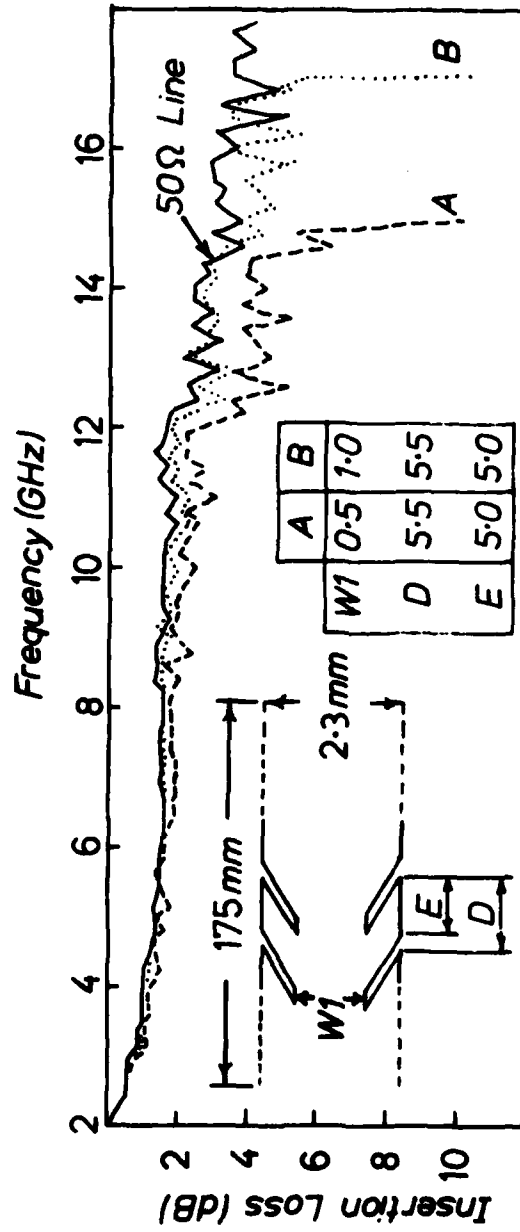
Fig 13: Measured insertion loss of serrated and conventional (50Ω) microstrip line. ϵ_r = 2.3

46
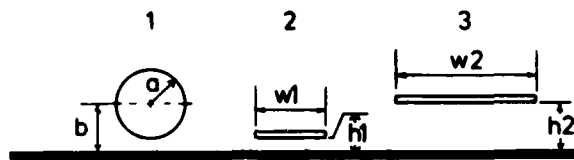
Round Wire 1	$\varepsilon_r=1$, $Zo=50\Omega$ $b/_a \approx 1\cdot4$
Microstrip 2	$\varepsilon_r=1$, $Zo=50\Omega$, $w/_h \approx 5$. For $h1\approx b-a$, $w1\approx 2a$.
Microstrip 3	$\varepsilon_r=1$, $Zo=50\Omega$, $w/_h \approx 5$. For $h2\approx b$, $w2\approx 4a$.

Fig 14: Round and flat conductors above a ground plane having the same (50Ω) impedance.

	FREQUENCY (GHz)	
	25	50
$Z_o(\Omega)$	50	50
a(mm)	2·0	1·0
b(mm)	2·74	1·37
h(mm)	0·74	0·37
w(mm)	3·7	1·85
$\propto_{cw} \frac{dB}{\lambda_o} \frac{o}{mm}$	0·017	0·024
$\propto_c \frac{dB}{\lambda_o} \frac{-}{mm}$	0·03	0·043

Table 6: Computed line loss for round and flat conductors above a groundplane (Cases 1 and 2 of Fig 14).

47
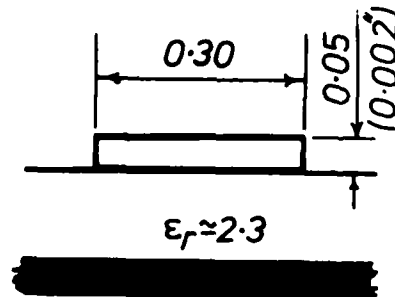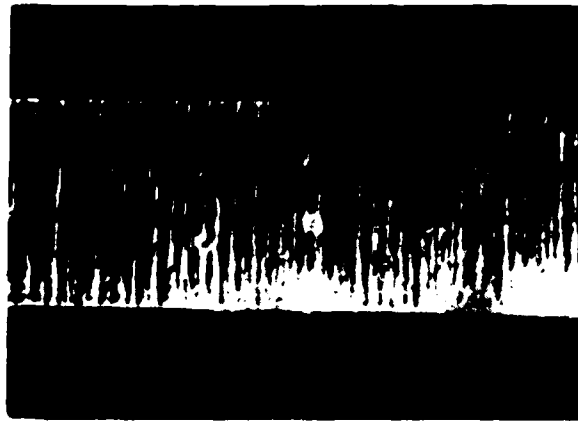
Unplated Microstrip Line.
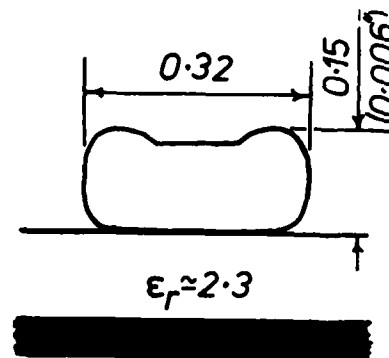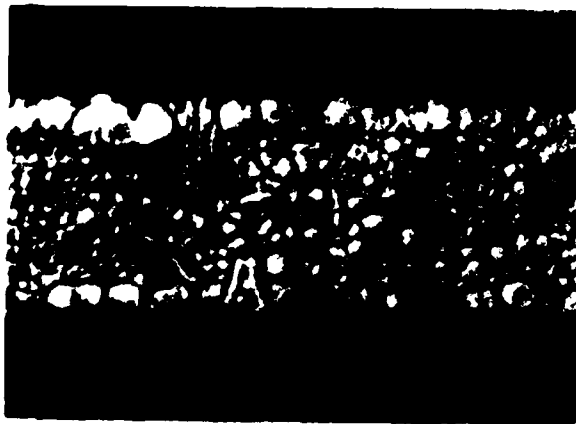
Electroplated Microstrip Line.

Substrate Thickness 0·127mm (0·005 inches)

Dimensions in millimetres.   Scale X 100.

Fig 15:   Photographs and details of the rounding of microstrip line
edges by electroplating

48

Comparisons made using 10cm microstrip lines
with E plane launchers. Frequency 90 GHz.

	Insertion Loss dB (typical)
Unplated Line	-10.8
Plated Line	-9.8

For $\varepsilon_{eff} \simeq 1.95$, $10cm/\lambda_m \simeq 42$.

Loss Reduction $\simeq 0.02$ dB/λ_m

Table 7: Measured loss reduction due to rounding of microstrip edges by plating

Fig 16: Photograph comparing the J-band and 90 GHz arrays and their associated E-plane transitions

50

23 dB Standard Horn.

——————— Co-polar.

——————— Cross-polar
with E-plane launcher.

·············· Cross-polar
with coaxial launcher.

-80 -70 -60 -50 -40 -30 -20 -10 0 +10 +20 +30 +40 +50 +60

Degrees.
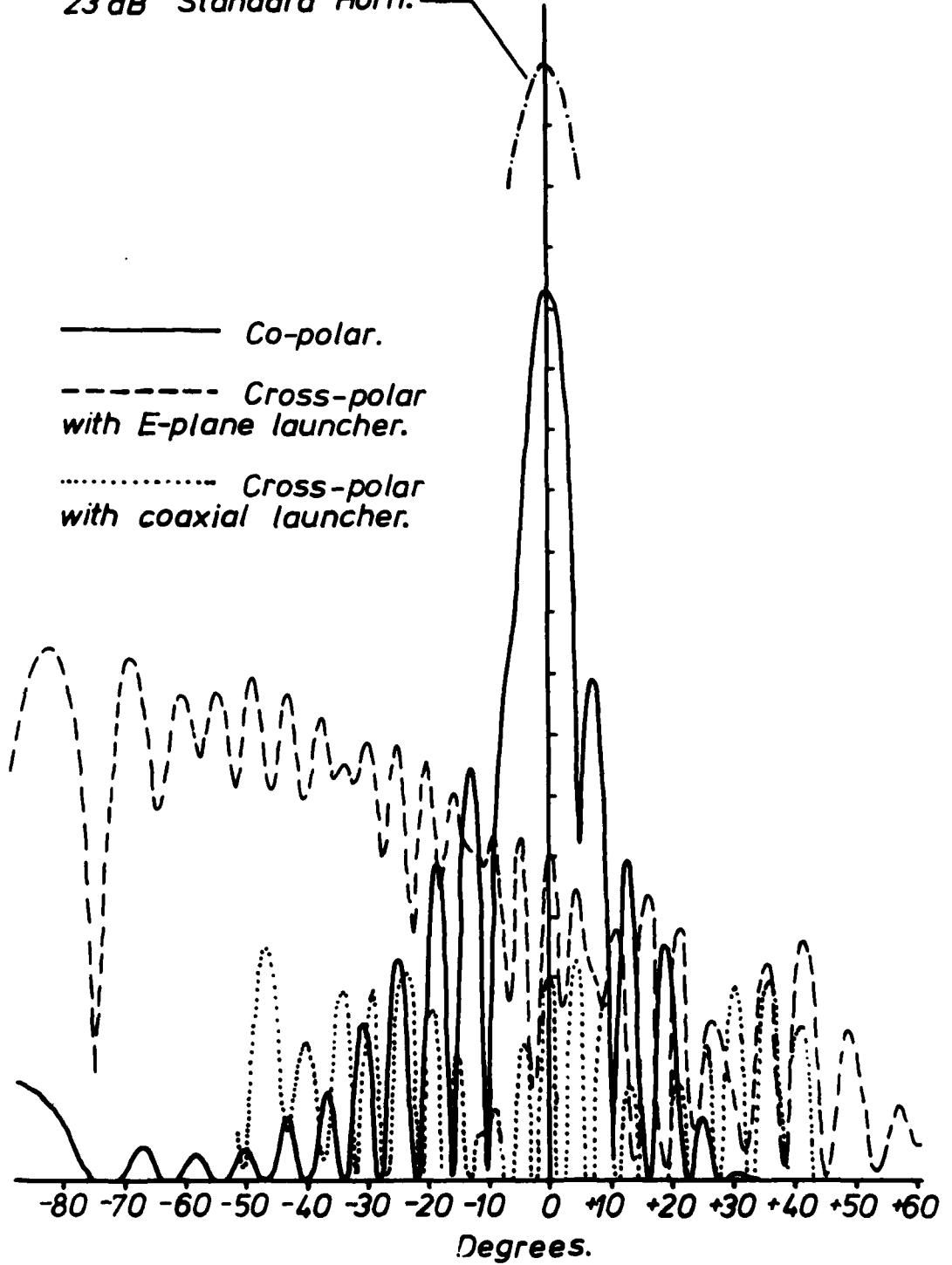
Fig 17: Radiation pattern of 32 element linear comb array with E-plane
launcher at 15.5 GHz

51

(a) Radiation

	Computed	Measured	
		15.5 GHz	91.4 GHz
Power Gain	20.65	15.6	12.0
Sidelobes (dB)	-13	-12	-9.0
Cross Polar (dB)	-	< -21	< -20
Input Reflection Coeff (dB)	-15.78	-13.5	< -20

(b) Losses

	15.5 GHz	91.4 GHz
Theoretical Gain (dB)	20.65	20.46
Measured Gain (dB)	15.6	12.0
Loss in launcher (dB) + lead in line	0.5 + 0.22 = 0.72	2 + 1.81 = 3.81
Mismatch loss (dB)	0.2	0.05
Actual Gain (dB)	16.5	15.86
Efficiency %	38.6	34.7

Table 8: Comparison of 32 element microstrip array performance at 15.5 and 90 GHz. The launcher is an E-plane type.
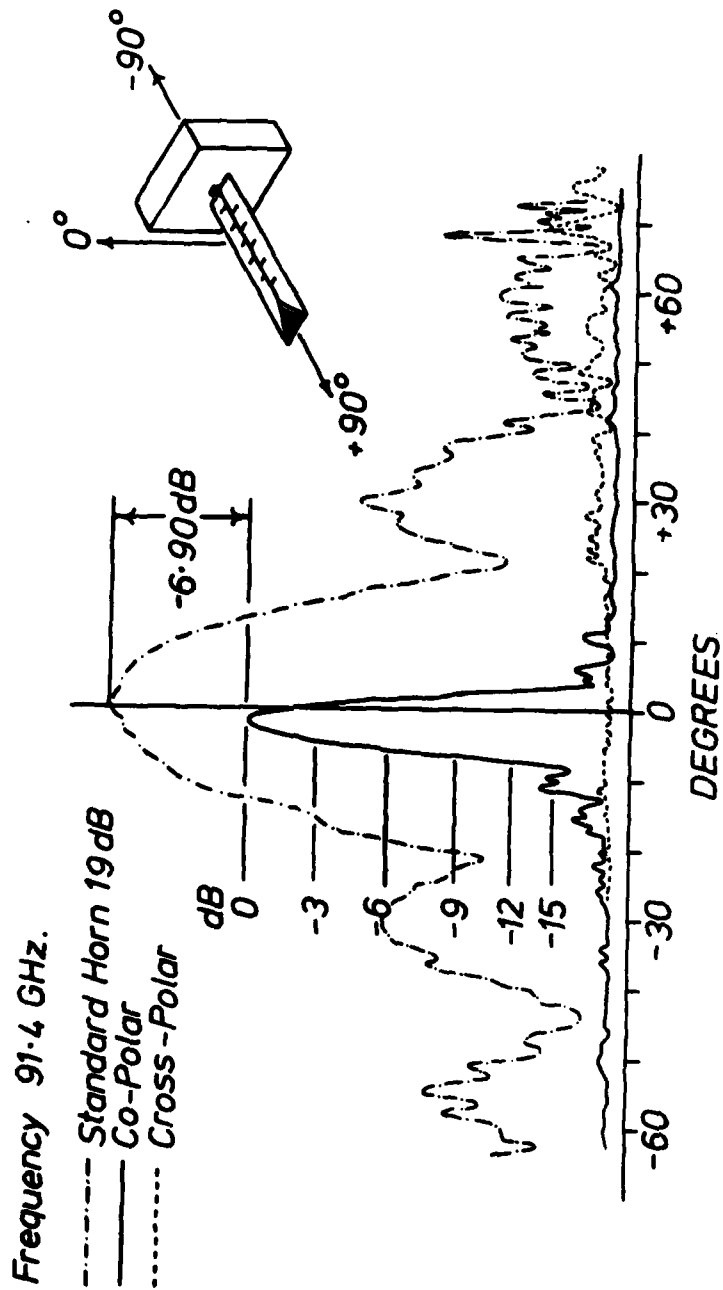
Fig 18: Radiation pattern of scaled 32 element linear comb array with E-plane launcher at 91.4 GHz

D = 2·29mm

0·25mm
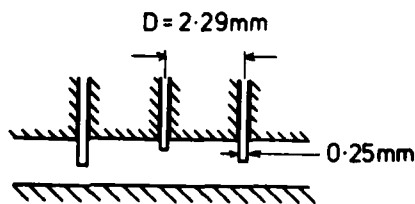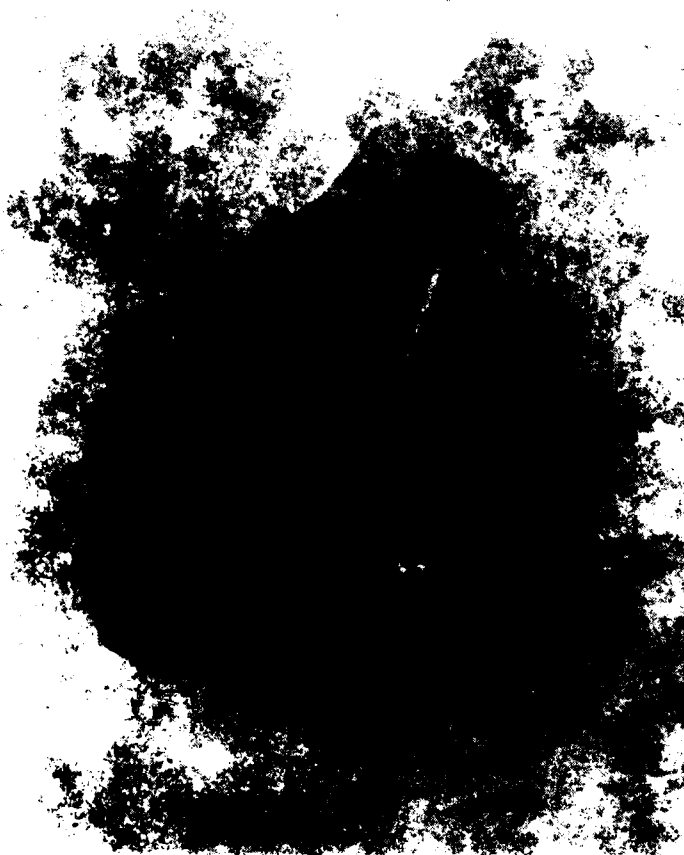
Fig 19: Photograph of 3-stub tuner + details of dimensions.

54

EFFICIENCY (%)

Directivity $\simeq 10\,\mathrm{Log}\; 4\pi\left[\dfrac{D}{\lambda_o}\right]^2$
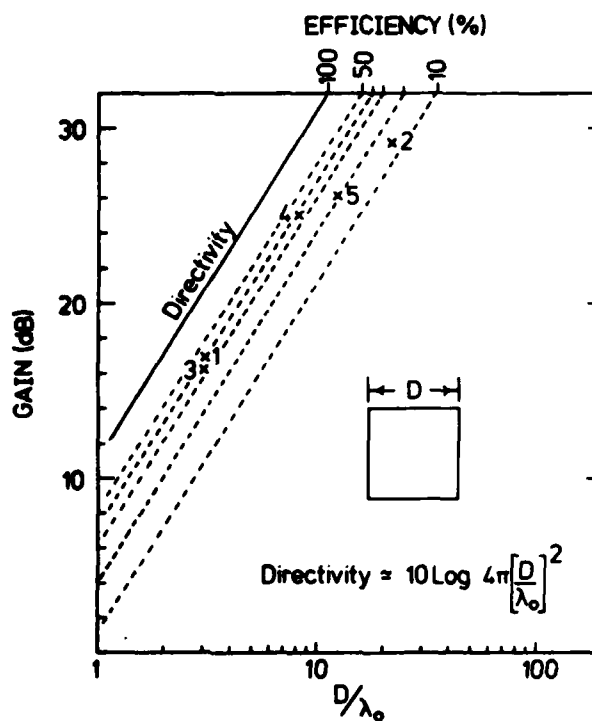
1. **Weiss** , 4 x 4 elements   (ref 47)   57.4 GHz

2. **Weiss** , 32 x 32 elements   (ref 47)   38.4 GHz

    (first two levels of power division replaced by waveguide)

3. **Williams** , 6 x 6 elements   (ref 48)   36.0 GHz

4. **Williams** , 16 x 16 elements   (ref 48)   36.0 GHz

5. **Williams** , 24 x 24 elements   (ref 48)   36.0 GHz

Fig 20: Comparison of measured gains of square microstrip patch arrays

55

(a)		
Frequency (GHz)	14.3	78.6
Resonator size (mm)	6.5 x 6.5	1.05 x 1.05
Assumed line loss (dB/λ_m)	0.1	0.14
Q_o calculated	275.8	195.0
Q_R calculated	19.1	24.3
Q_T calculated	17.9	21.6
Efficiency (%)	93.5	88.9
Q_T measured	28.2	43.7
Q_R*	31.4	56.3
Efficiency (%)	89.8	77.6

*Calculated from measured Q_T and calculated Q_o value.

(b)
$$\frac{1}{Q_T} = \frac{1}{Q_o} + \frac{1}{Q_R}$$

$$\text{Radiating Efficiency} = Q_T/Q_R \times 100\%$$

$$Q_R = \frac{\pi}{4G_r Z_m} \text{ where } G_r = \frac{\omega_c^2}{90\lambda_o^2} \qquad (\omega_c < 0.35\lambda_o)$$

$$\text{and } \omega_c = \frac{120\,\pi h}{\sqrt{\epsilon_r}\,Z_m} \quad (\text{ref 29})$$

$$Q_o = \frac{\pi}{\lambda m(\alpha)} \ (\text{ref 6})$$

Table 9: Example of patch efficiency at ~ 79 GHz compared to microwaves
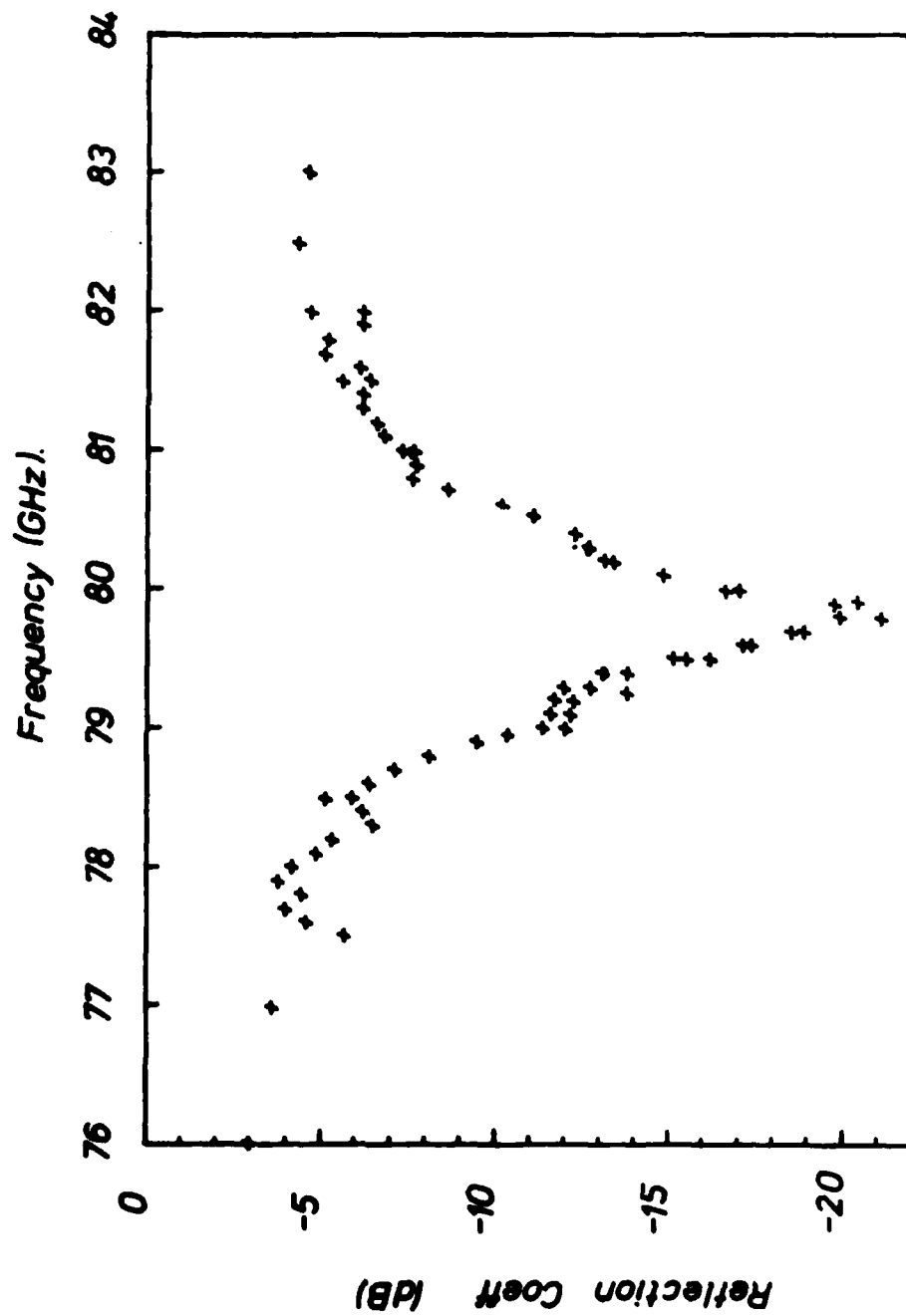
Fig 21(a): Reflection measurement on microstrip patch for extraction of Q value from frequency by frequency measurements with a power meter. 5880 RT-DUROID with ½ ounce rolled copper.

(c)

(b)
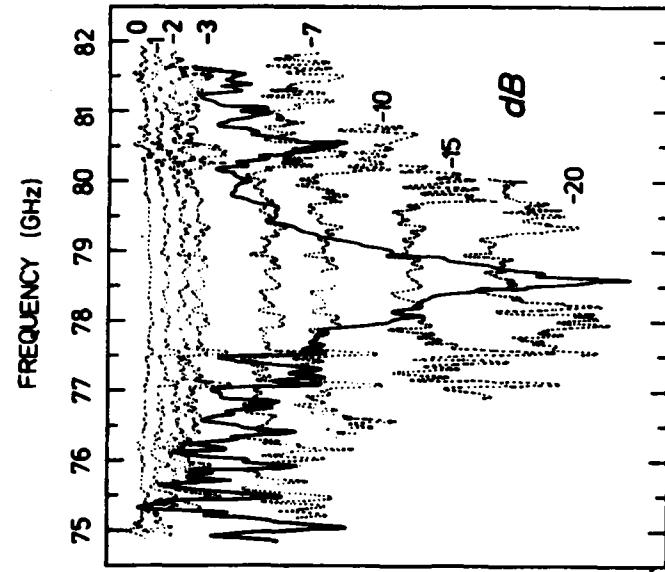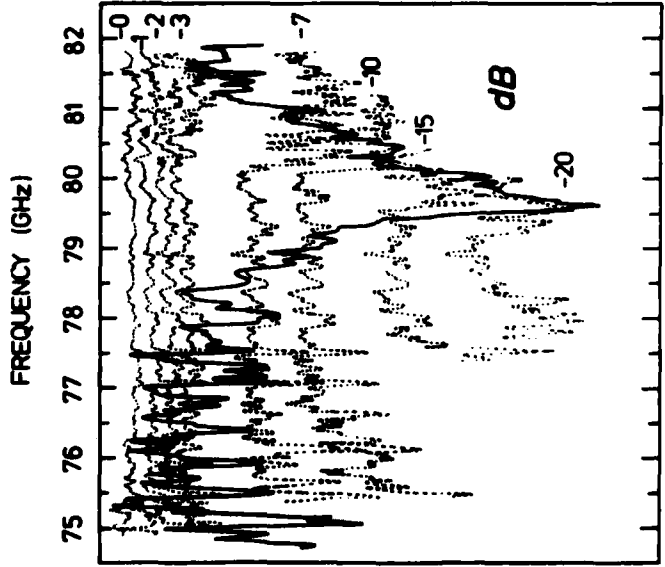
Swept frequency, reflection Q measurements on square
patch resonators with an E-plane transition

Fig 21(b): 5880 RT-DUROID with ½ ounce rolled copper
            r = 2.2, h = 0.127 mm

Fig 21(c): 5870 RT-DUROID with ½ ounce electrodeposited copper
            r = 2.3, h = 0.127 mm

------- reference,   ———— patch response

58

Fig 21(d): Photograph of E-plane launcher with patch resonator.

Number of Elements	D/λ_0	Directivity (dB)	Measured Gain (dB)	Mismatch Loss (dB)	Patch Loss (dB)	Est Line Loss (dB)	Radiation Loss (dB)	Launcher Loss (dB)
4	1·18	12·43	10·7	~0	0·46	0·16	1·33	0·24
16	2·96	20·33	15·1	0·6	=	0·41	3·98	=
64	6·44	27·17	20·1	0·45	=	0·90	5·48	=
256	13·45	33·57	—	—	=	1·88	6·98	=
1024	27·47	39·77	—	—	=	3·81	8·48	=
4096	55·50	45·90	—	—	=	7·78	9·98	=
16384	111·59	51·94	—	—	=	15·65	11·48	=

Number of Elements	Total Feeder Loss (dB)	Measured Gain (dB)	Predicted Gain (dB)	Efficiency (%)
4	2·19	10·7	10·24	67·1
16	5·09	15·7	15·24	34·4
64	7·08	20·55	20·09	21·8
256	9·56	—	24·01	11·1
1024	12·99	—	26·78	5·0
4096	18·46	—	27·44	1·4
16384	27·83	—	24·11	0·2
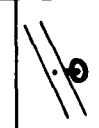
	Estimated Radiation Loss (dB)
	0·58
	0·75
	0·24

Table 10: Gain and loss budget for square arrays of microstrip patch elements. Measurements at 13.9 GHz, ϵ_r = 2.3, h = 0.787mm.

60
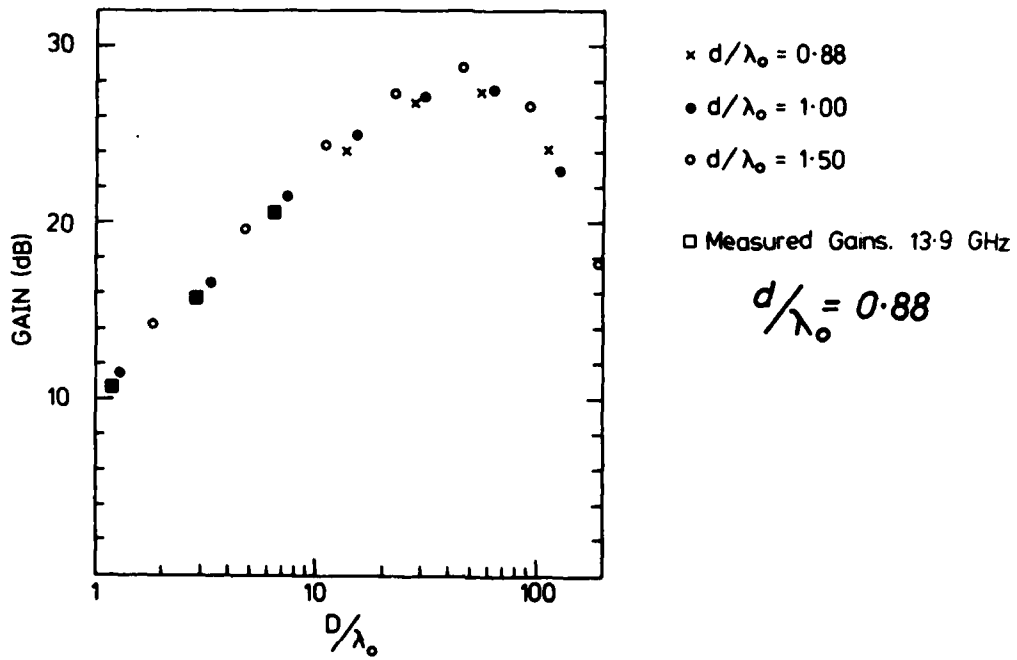
Fig 22: Measured and predicted relationship between array gain and size for different element spacing and hence line lengths. Radiation from T-junctions and bends are also included.
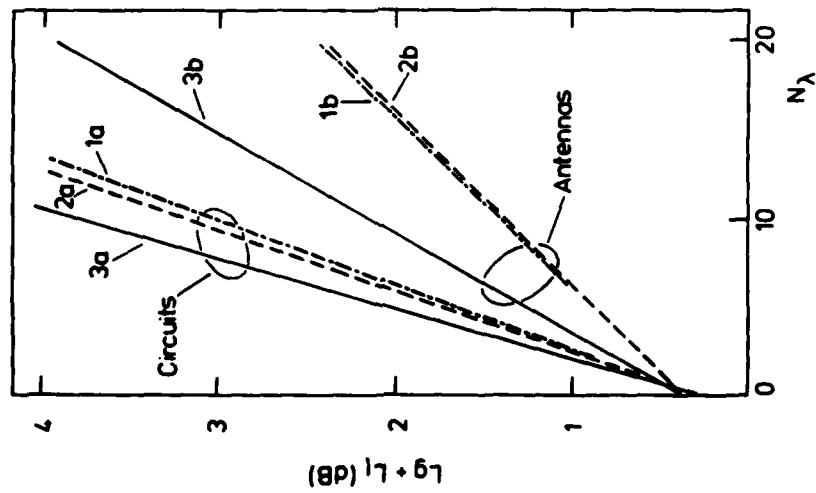
1a $h = 0.017\lambda_o$	$\epsilon_r = 2.32$	$\tan\delta = 0.001$	$\Delta = 0.005mm$
1b $h = 0.041\lambda_o$	$\epsilon_r = 2.32$	$\tan\delta = 0.001$	$\Delta = 0.005mm$
2a $h = 0.009\lambda_o$	$\epsilon_r = 3.8$	$\tan\delta = 0.0001$	$\Delta = 0.005mm$
2b $h = 0.032\lambda_o$	$\epsilon_r = 3.8$	$\tan\delta = 0.0001$	$\Delta = 0.005mm$
3a $h = 0.005\lambda_o$	$\epsilon_r = 10$	$\tan\delta = 0.001$	$\Delta = 0.005mm$
3b $h = 0.02\ \lambda_o$	$\epsilon_r = 10$	$\tan\delta = 0.001$	$\Delta = 0.005mm$

Fig 23: Microstrip system losses (50Ω lines) at 90 GHz for circuit and antenna feeder applications.
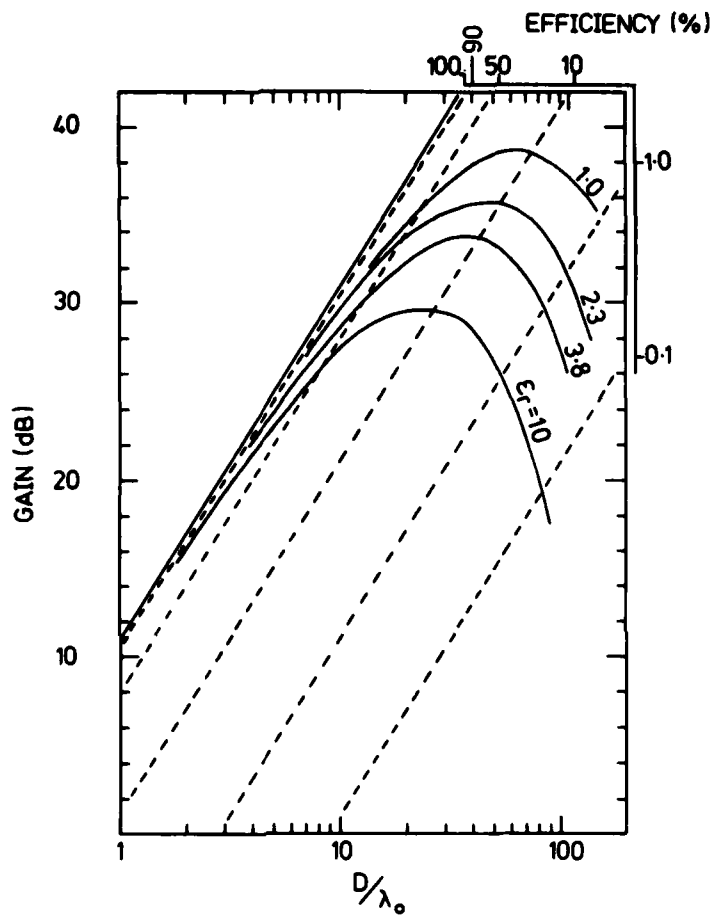
Fig 24: Graph of the effect of substrate dielectric constant on the maximum broadside gain obtainable from square linear array antennas assuming a feeder line (50Ω) loss of 0.13dB per guide wavelength. Corporate feed and radiation losses are omitted.

63
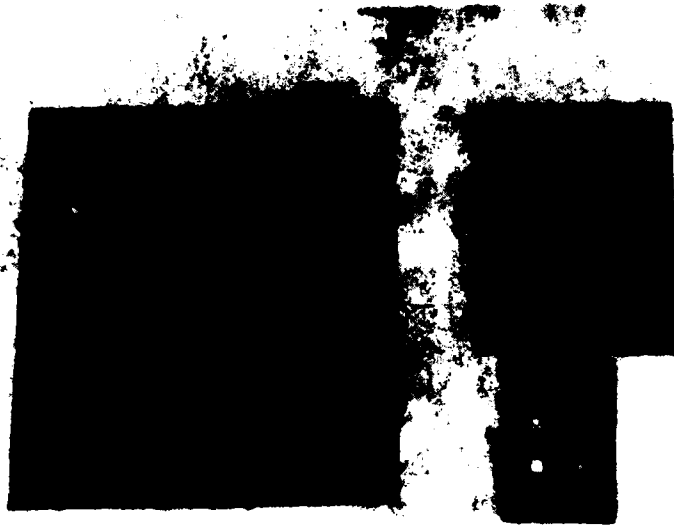
Fig 25: Photograph of patch arrays used in measurements at microwaves
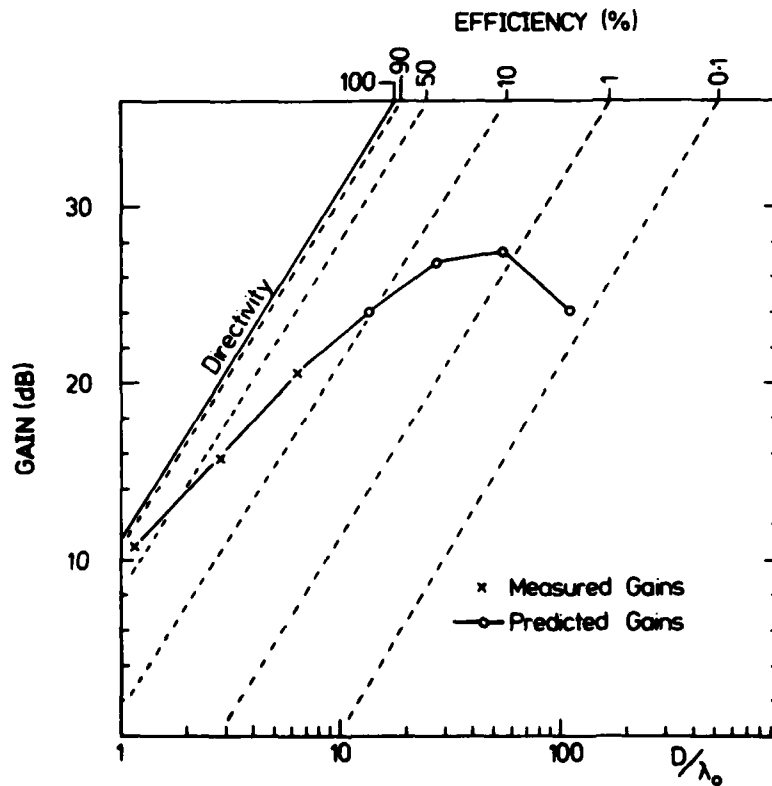
Fig 26: Gain and efficiency predictions for patch arrays at 13.9 GHz
$h = 0.787mm, \varepsilon_r = 2.3$.

Efficiency (%)

80

100 50 10 1·0 0·1

30

GAIN (dB)

20

10

0

Predicted Gains

× Measured Gains 78·5 GHz.

1 10 100 D/λₒ
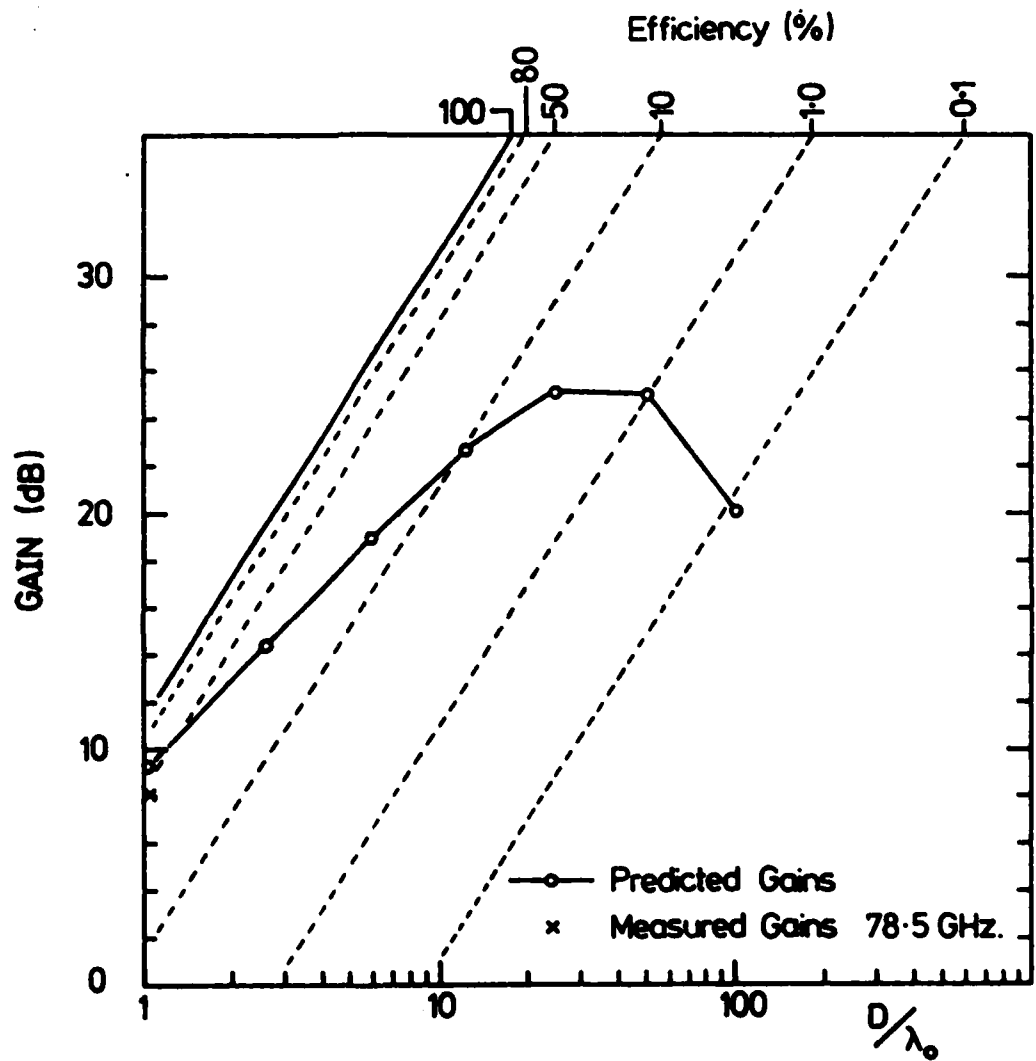
Fig 27: Gain and efficiency predictions for patch arrays at 80 GHz.
Line loss 0.13 dB/λₘ, h = 0.127mm, εᵣ = 2.3.

65

System	Gain	Efficiency	Bandwidth	Patch Antennas (parallel fed)	Linear Antennas (comb, report, etc)
Radar	High > 30dB	High > 80%	Depends on application	Efficiency too low at high gain	Efficiency a problem - low loss feeder needed.
Radiometry	High > 30dB	High	Wide	Efficiency too low. Bandwidth limited.	Efficiency too low. Bandwidth limited.
Seekers	~ 30dB	Not critical	Depends on application	Possible. Efficiency low. No squint.	Large corporate feed needed. Beam squints with freq.
Submunitions	Not critical	Not critical Depends on application	Not critical	Well suited. 80GHz Gain ~25 dB. Efficiency ~ 5%. Circular polarization possible.	Probably too long. Requires additional corporate feed for 2D array.
ECM Expendable and non expendable	Low	High	Wide	Efficiency a problem. Possible.	Bandwidth and efficiency a problem.
ESM	Low	High	Wide	Efficiency a problem. Possible.	Bandwidth and efficiency a problem.
Communications	High Depends on Power budget	High	Wide	Possible. Efficiency a problem. Circular polarization possible.	Possible.

System	Gain	Efficiency	Bandwidth	Patch Antennas (parallel fed)	Linear Antennas (comb, rampart, etc)
Aircraft to satellite	Medium	High	Wide	Possible. Circular polarisation possible.	Possible. Circular polarisation possible with rampart arrays.

Table 11: Compatibility of patch and linear arrays with typical military requirements.

66b
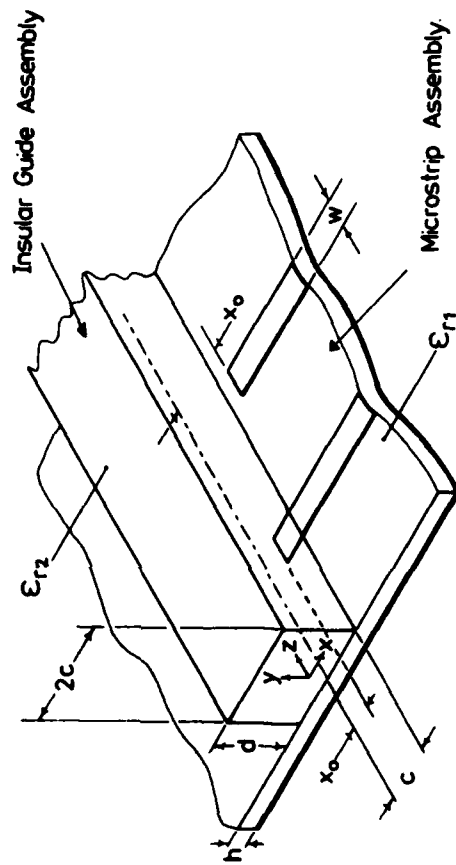
Fig 28: Coupling of microstrip line to insular guide.
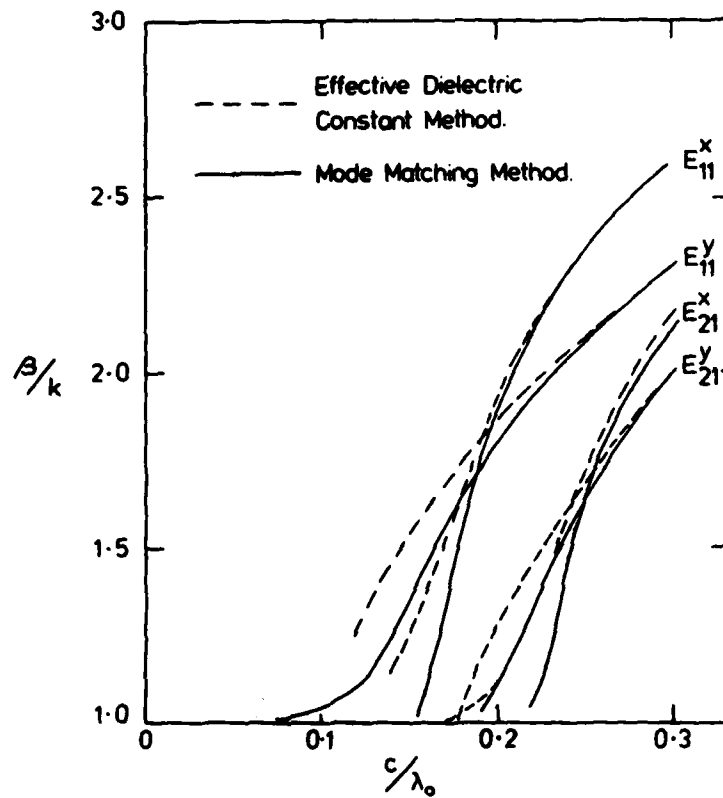
Fig 29: Computed mode chart for insular guide. $\varepsilon_{r1} = 2.3$, $\varepsilon_{r2} = 10$, $h = 0.242d$, $c = 1.58d$.
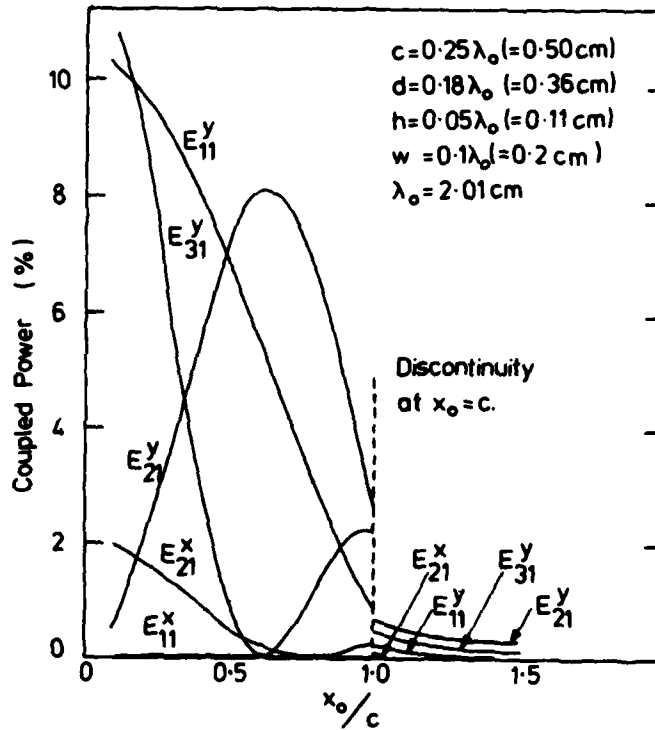
Fig 30: Coupling between insular guide and microstrip line as a function of the distance from the centre of the guide.

Coupled Power (%) vs w/λ_o

$c = 0.25\lambda_o \, (= 0.50\,\text{cm})$
$d = 0.18\lambda_o \, (= 0.36\,\text{cm})$
$h = 0.05\lambda_o \, (= 0.11\,\text{cm})$
$x_o = 0.1c \, (= 0.03\lambda_o)$
$\lambda_o = 2.01\,\text{cm}.$
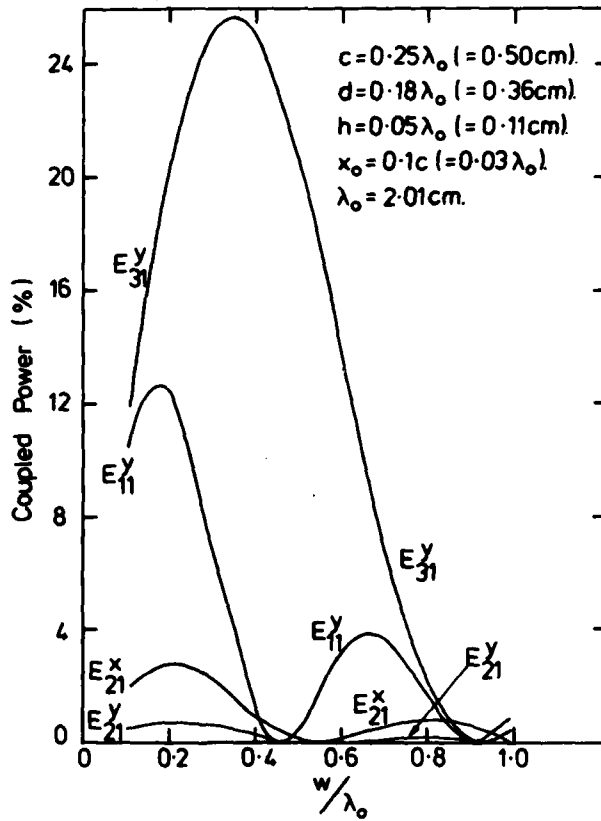
Fig 31: Coupling between insular guide and microstrip line as a function of strip width.

70
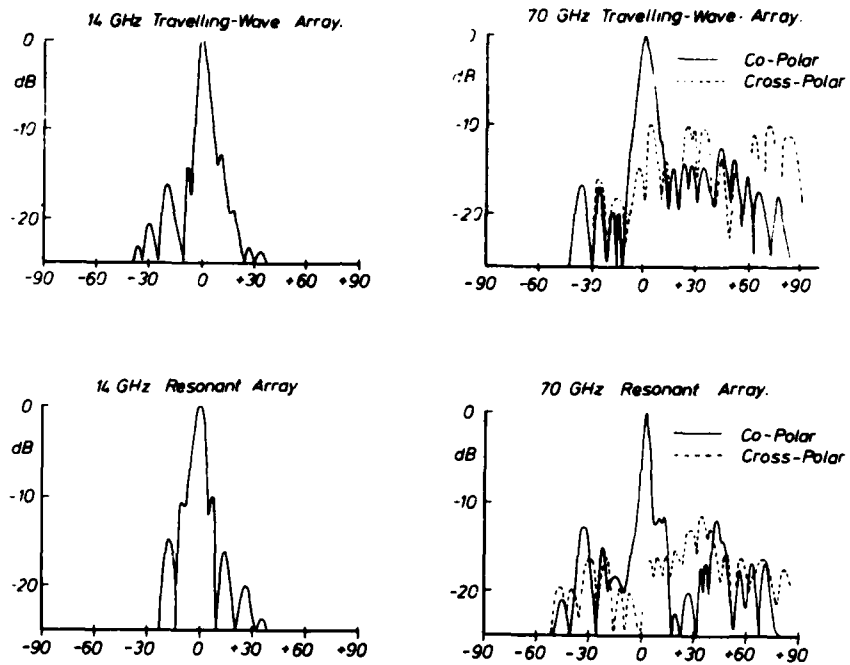
	Microwave	Millimetre
ε_{r1}	2·3	2·3
ε_{r2}	10·5	10·5
c (mm)	4·29	0·69
d (mm)	2·86	0·46
x_0/c	1	0·87
h (mm)	0·787	0·127

Fig 32: Radiation patterns of hybrid arrays of narrow stubs utilizing the E_{21}^{x} mode.

71
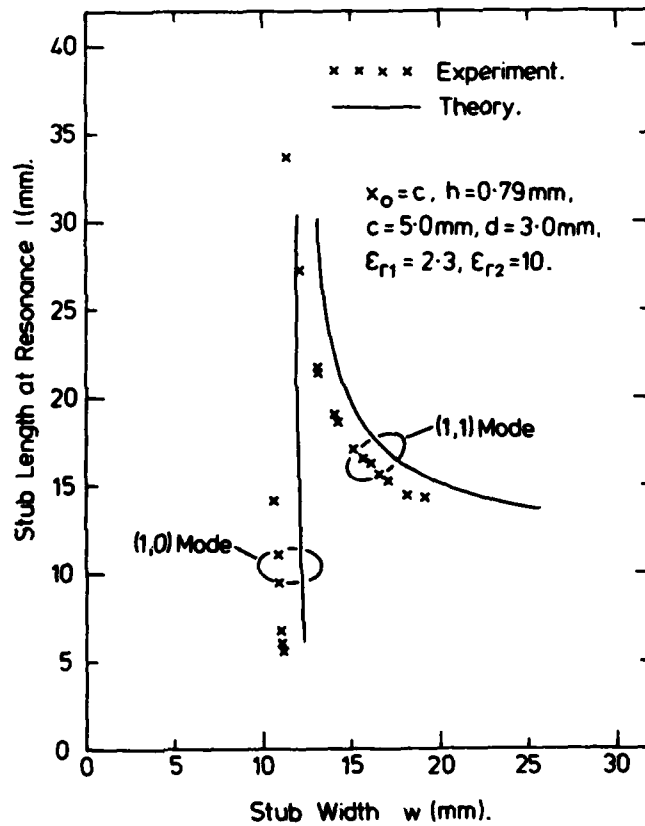
Fig 33: Transcendental equation relationship between stub width and length.
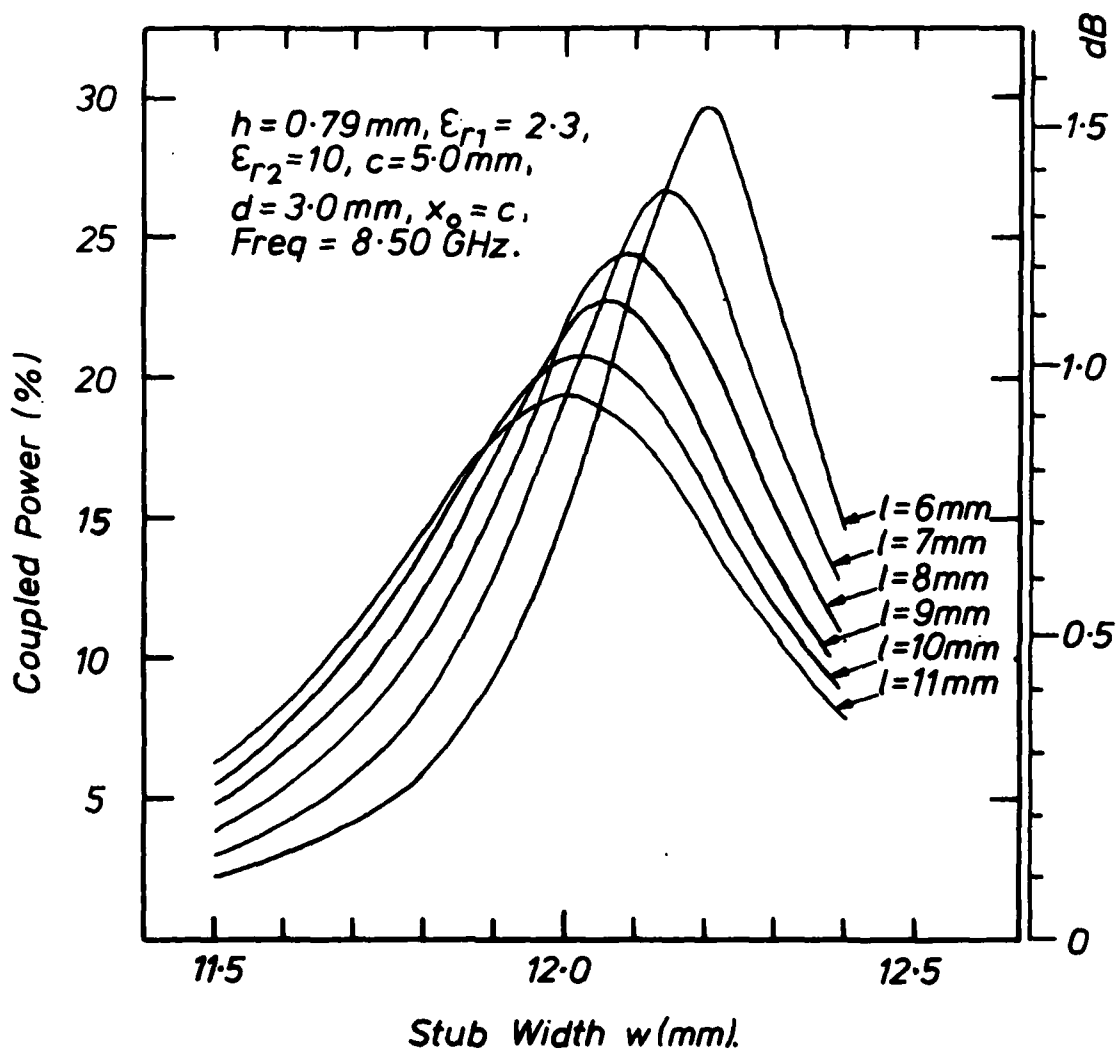
Fig 34: Computed power coupling levels for (1,0) mode in microstrip patch as a function of length l.
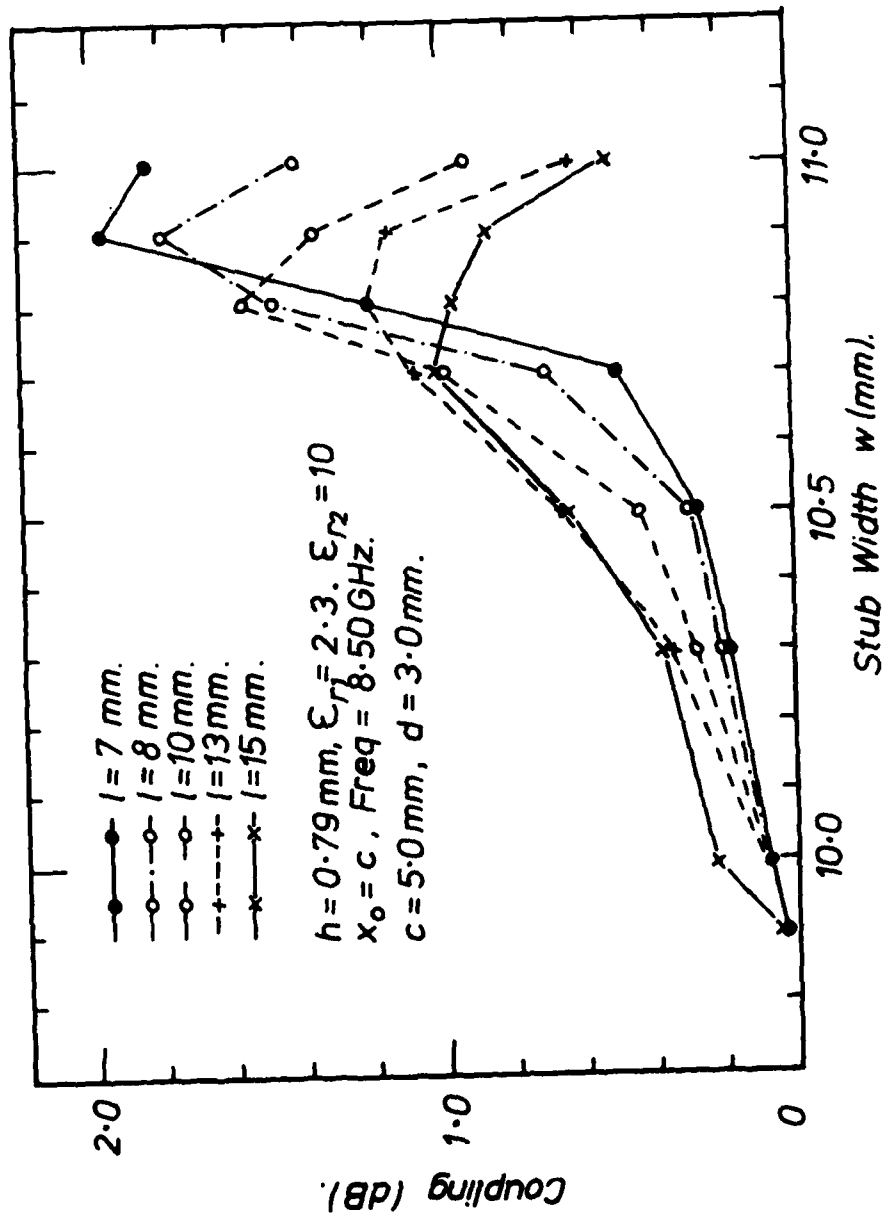
Fig 35: Measured power coupling levels for (1,0) mode in microstrip patch as a function of length ℓ.
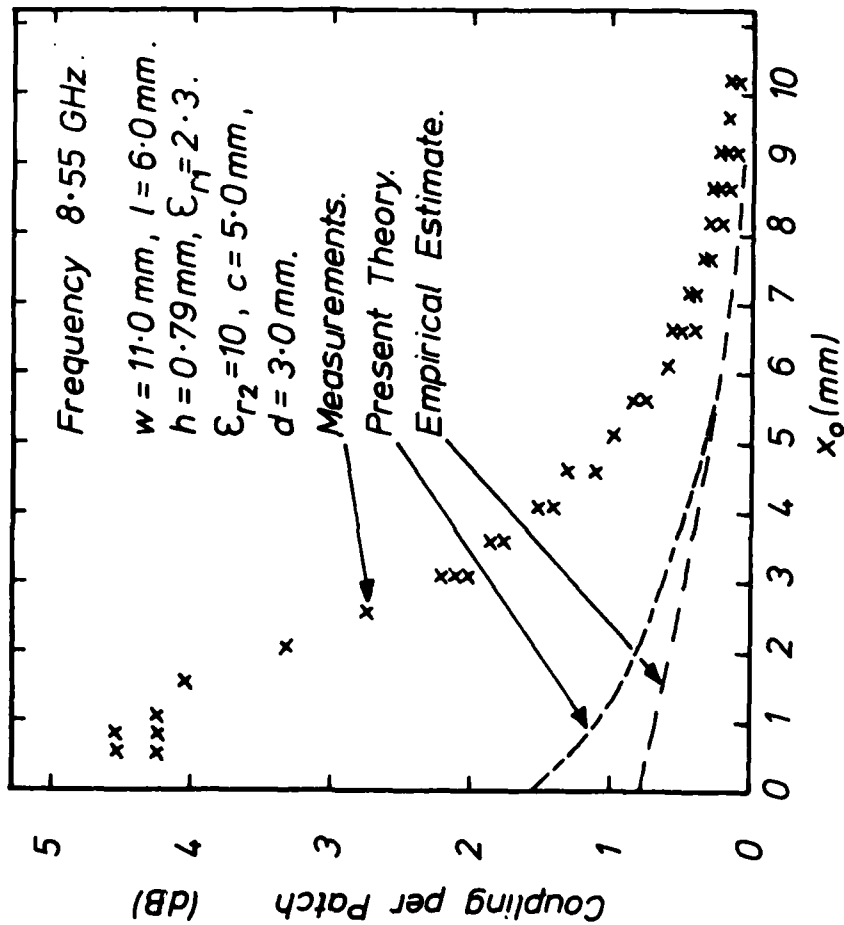
Fig 36: Coupling levels to microstrip patch as a function of separation x_o for $\ell = \lambda_m/4$.

75
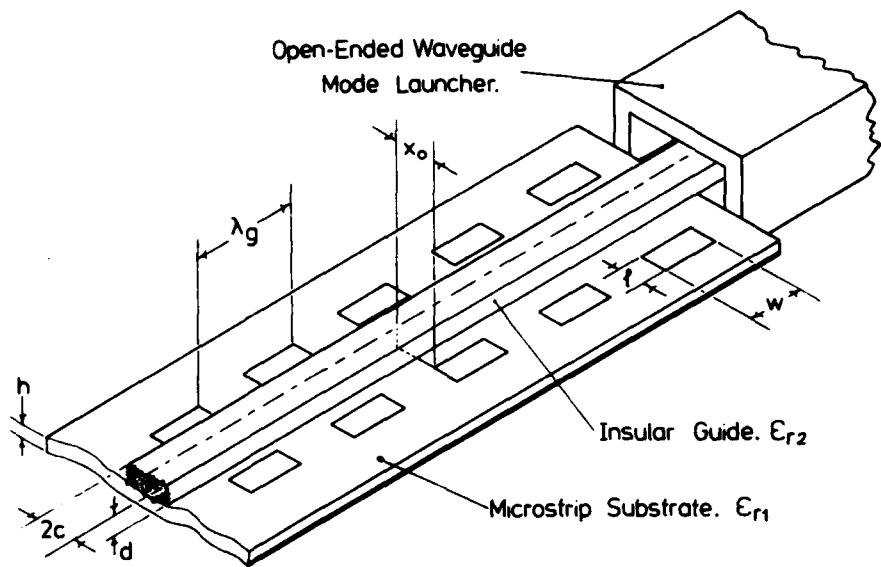
Fig 37: Layout of hybrid array.
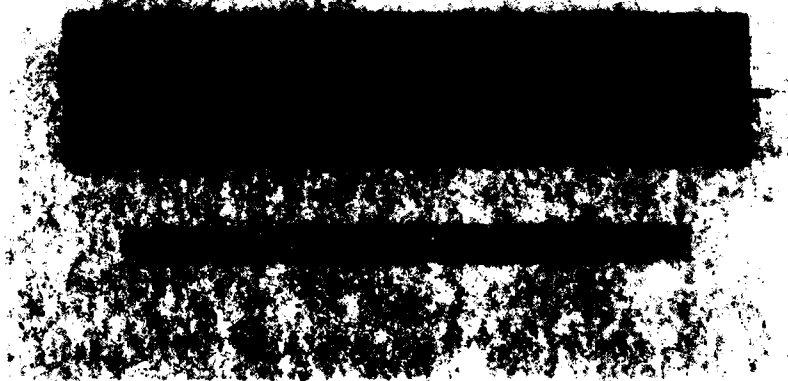
Fig 38: Photograph of the 90 GHz, 80 element hybrid array.

76

Frequency	90.00 GHz
Beamwidth (theory)	2.15^{o}
(measured)	2°
Squint angle	$+16^{o}$
Sidelobes	-9.0 and -11.2dB
Cross-polar	< -25dB
Directivity (theory)	24.2dB a.
Gain (measured)	17dB
Launcher loss (theory)	2dB
Mismatch loss (measured) (ρ < -20dB)	0.04dB
Feeder loss (theory)	2dB b.
Resonator loss (measured)	0.97dB c.
Load loss	2.19dB d.

Efficiency (Assuming no launcher or load loss)	50.0%	e.
Efficiency of microstrip array of same physical length	24.9%	f.

a.   Directivity = $10 \log (\frac{A}{\lambda_o^2}) \times \cos$ (squint angle) dB.

b.   Feeder loss calculated using 0.05dB/λ_g over 40 wavelengths.

c.   From measurements on patch resonator Q's (see 5.2).

d.   Load loss = 24.2 - [17 + 2 + 0.04 + 2 + 0.97] = 2.19dB.

e.   Efficiency = 24.2 - [17 + 2 + 2.19] = 3.01dB $\cong$ 50.0%.

f.   Microstrip feeder of same physical length (39 wavelengths, $\epsilon_{eff} \simeq 2$, $Z_m = 50\Omega$, Line loss 0.13dB/λ_m). Patch loss $\simeq$ 0.97dB.
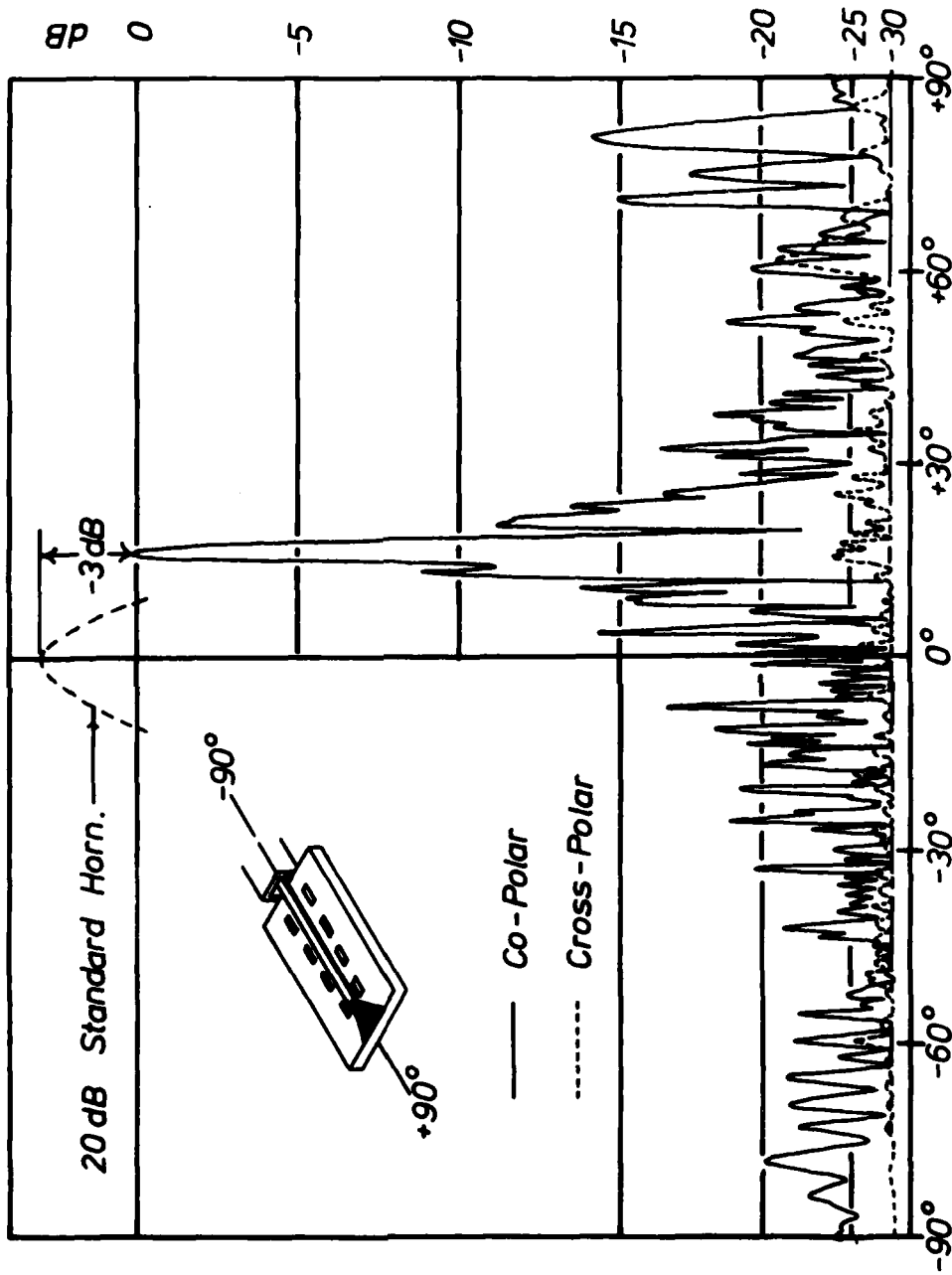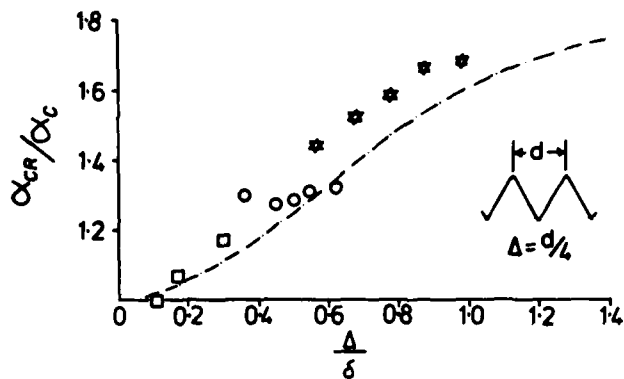
Table 12: Hybrid array power budget

Fig 39: Radiation pattern of hybrid antenna polarised with its E-plane parallel to the feed axis. (Frequency 90.00 GHz, 40 elements per side, length 92.3 mm, C = 0.55 mm, d = 0.35 mm, h = 0.127 mm, ε_{r1} = 2.3, ε_{r2} = 10, w = 0.995 mm*, l = 0.497 mm*, x_{omax} = 0.29 mm, x_{omin} = 0.18 mm, Standard horn gain ∿ 20dB. *average value.)

Fig A1: Theoretical and experimental variation of microstrip excess
         attenuation against the ratio of r.m.s. surface roughness over
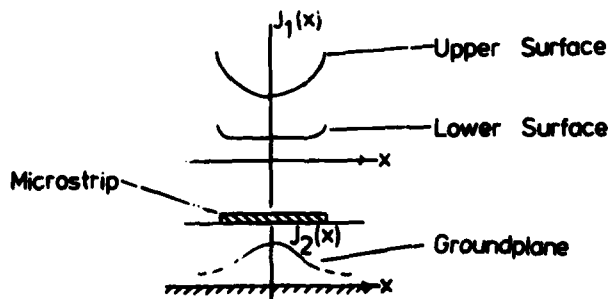   the skin depth.

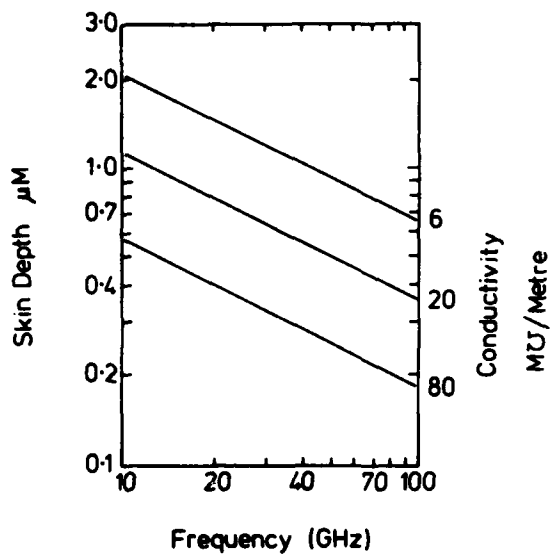Fig A2: Microstrip surface current density distribution.
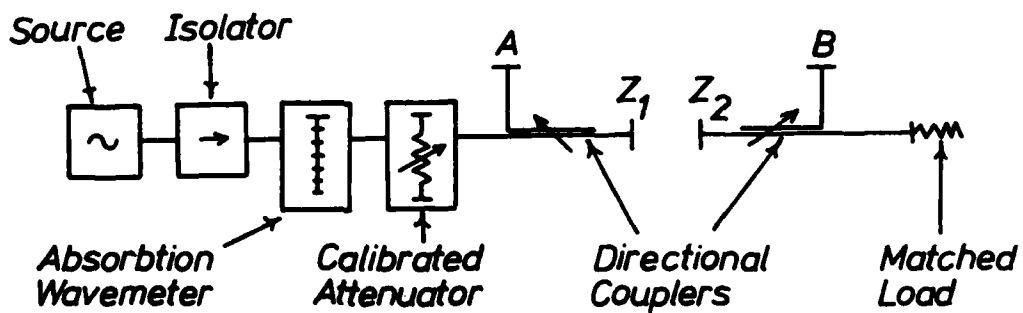
Fig A3: Variation of skin depth with frequency.

Fig A4: Schematic of apparatus used in line loss measurements.